World Electric Vehicle Journal

MDPI

Article

Stochastic Utilization Model for Electric Vehicle Charging Stations: A Proof-of-Concept Approach for Residential and Public Charging Stations

Matej Tkac [1,*], Filip Petrík [1,*], Marek Höger [1] and Partha Kayal [2]

[1] Department of Power Systems and Electric Drives, Faculty of Electrical Engineering and Information Technology, University of Žilina, Univerzitná 8215/1, 01026 Žilina, Slovakia
[2] Department of Electrical Engineering, National Institute of Technology Silchar, Silchar 788010, Assam, India
* Correspondence: matej.tkac@uniza.sk (M.T.); filip.petrik@feit.uniza.sk (F.P.)

Abstract

The increasing adoption of electric vehicles (EVs) creates a need for realistic charging-station utilization scenarios to support studies of distribution-network impacts and charging-management strategies. This paper presents a proof-of-concept stochastic framework for simulating EV connection events, plugged-in durations, and station occupancy at 15-min resolution using historical charging-session records. Connection counts are generated from time-dependent Poisson distributions with rates estimated for each quarter-hour interval separately for workdays and weekends. Connection durations are sampled from empirical distributions conditioned on arrival time, while the available number of charging points constrains simultaneous occupancy. The same modeling workflow is applied without structural modification to two publicly available datasets representing residential charging in Trondheim, Norway, and public charging in Palo Alto, California, USA. In calibration-period consistency checks, the two-sample Kolmogorov–Smirnov statistics for distributions of quarter-hourly connection totals are $D = 0.052$ for the residential case and $D = 0.083$ for the public case. These results indicate close agreement in the distributions of aggregated connection counts within the fitted periods but do not establish predictive accuracy on unseen data. The proposed approach provides a reproducible procedure for constructing site-specific stochastic charging-station occupancy scenarios that can support subsequent evaluations of charging coordination and energy-management methods. Its present scope is limited to connection behavior and occupancy; active charging power, out-of-sample performance, and responses to changes in surrounding infrastructure require separate modeling or validation.

Keywords: electric vehicle; probability distribution function; residential charging station; public charging station; stochastic model

Academic Editor: Kan Akatsu

Received: 28 September 2026
Revised: 18 November 2026
Accepted: 19 November 2026
Published: 25 November 2026

Copyright: © 2026 by the authors. Published by MDPI on behalf of the World Electric Vehicle Association. Licensee MDPI, Basel, Switzerland. This article is an open access article distributed under the terms and conditions of the Creative Commons Attribution (CC BY) license.

1. Introduction

Nowadays, we are witnessing a significant increase in the number of electric vehicles (EVs) being used in transportation. The motivation for using EVs is undoubtedly their low carbon footprint and improved air quality in densely populated areas due to reduced

emissions. Another important factor contributing to the increasing popularity of EVs is the development of the public charging infrastructure [1]. Powering EVs with electricity generated from renewable sources leads to a relatively low-emission form of transportation, thereby contributing to a reduction in overall environmental impacts [2–4].

However, the increasing number of EVs means that these vehicles need significant amounts of electrical energy to charge their batteries (depending on the state of charge) via charging stations [5]. This brings new challenges for distribution system operators. Therefore, many authors focus in their papers on predicting energy consumption caused by EV charging. For instance, authors of [6] proposed a spatial load forecasting method to predict the spatial distribution and grid impact of EV charging demands in urban areas. Authors of [7] used time-series and machine learning approaches to predict electric vehicle load.

In the near future, some measures will be necessary to avoid problems in the distribution grid, such as overloading of the transmission elements, undervoltage events, or problems with power factor and harmonic distortion. While it will eventually be necessary to physically upgrade certain parts of the distribution system, the negative impacts on the distribution grid can be significantly mitigated through the appropriate coordination of individual charging stations [8]. However, the development, testing, and operation of such advanced coordination strategies require reliable and accurate modeling of charging station behavior [9]. Realistic charging scenarios are likewise an input to infrastructure-planning and traffic-informed design and operation studies of charging stations in distribution grids [10,11]. The most challenging aspect of EV charging station behavior modeling is the stochastic nature of its operation. However, most studies focused on smart control and coordination of EV charging stations are developed and tested on highly simplified models.

Methods used for the testing of new control algorithms involve defining the times of connection and disconnection to and from the charging stations at the authors' discretion, as in refs. [12–14], or using data obtained from surveys to estimate the appropriate values as in refs. [15,16]. However, to create and utilize charging station operation models that could be used to test proposed mechanisms more comprehensively, it is important to utilize the historical charging data of the charging station operation for a realistic representation of charging station operations. To this end, it is imperative to develop complex models capable of accurately representing the charging station operation based on historical data, as in refs. [17–19].

In the current literature, various stochastic methods and approaches are employed to represent charging station utilization in models. For instance, the authors of [17] used probability distributions of EV arrival time, charging duration, and energy consumption to create charging profiles for fast-charging stations using data collected from fast-charging stations in the Netherlands. In papers [20,21], the Poisson distribution was applied to model EV utilization. Specifically, in ref. [20], the Poisson distribution modelled EV motion within a microgrid, incorporating factors such as EV routes and motion probabilities to estimate arrival rates at the charging station. In ref. [21], the Poisson distribution was employed to represent the arrival times of electric taxis and other EVs at the fast-charging station, whereas a normal distribution was used for modelling the duration of charging services, based on survey data analysis. To predict EV arrival and departure times, ref. [19] employed a stationary probability distribution. Beyond probability distributions, other methods have been explored in the literature. For instance, Markov chain models were used in [18] and [22] to predict and estimate EV usage based on historical data. The authors in [18] utilized the Markov model to predict EV availability at charging stations based on historical data, whereas ref. [22] used a combination of

Markov chain and Monte Carlo method to estimate the impact of EVs on a medium voltage network.

Compared with existing approaches, the main contribution of the proposed methodology lies in integrating time-dependent stochastic connection generation, arrival-time-conditioned connection durations, and charging-station capacity constraints within a unified simulation framework. The methodology requires historical connection and disconnection timestamps and information about station capacity, without requiring detailed vehicle trajectories, user surveys, or charging-power measurements. Its implementation relies on relatively simple probability distributions and empirical data matrices, making it adaptable to different charging environments. Unlike approaches explicitly modeling charging power or more complex temporal dependencies, the proposed method focuses on reproducing connection behavior and station occupancy. This simplicity comes at the expense of not explicitly capturing energy consumption, unserved demand, or longer-term behavioral changes.

This paper presents a proof-of-concept stochastic charging-station utilization model capable of representing the utilization of electric vehicle charging stations at 15-minute resolution. Rather than predicting individual drivers' decisions or grid power directly, it generates connection starts and plugged-in connection durations using distributions estimated from recorded sessions for a realistic representation of charging patterns. The primary objective is to demonstrate that the proposed methodology can be successfully applied to construct charging station utilization models from arbitrary historical datasets, thereby enabling accurate simulation of both residential and public charging station behavior. Moreover, this paper presents and describes the methodology utilized for the construction of the presented charging station utilization models. To demonstrate the versatility of the proposed approach, the functionality of the proposed charging station utilization model and the proposed methodology is validated using two distinct publicly available charging datasets: a residential charging dataset from Norway and a public charging dataset from Palo Alto, California, USA.

The 15-min temporal resolution employed in this study was selected primarily to align the proposed charging station utilization model with the quarter-hourly intervals commonly used in electrical grid analyses, load profiling, and electricity market settlement. Furthermore, this resolution provides a practical compromise between the temporal representation of charging station behavior and computational complexity, particularly given the proof-of-concept nature of this study. Although the proposed methodology is not inherently restricted to 15-min intervals, its application at finer temporal resolutions, such as 1 or 5 min, requires sufficiently detailed historical charging data to ensure reliable estimation of the underlying probability distributions. Additionally, finer temporal discretization increases the dimensionality of the input matrices and computational demands, while potentially affecting the statistical robustness of the model. Consequently, the present study focuses on 15-min resolution, although the proposed methodology remains applicable to finer temporal resolutions, provided that suitable historical data are available and the resulting models are appropriately validated.

The main contributions of this paper can be summarized as follows. First, a general-purpose stochastic charging station utilization model operating at 15-min resolution is proposed, capable of simulating charging station behavior over arbitrary simulation periods and for charging stations of varying sizes. Second, a systematic and transferable methodology for constructing such models from historical charging data is presented, encompassing dataset preparation, matrix construction, probability distribution identification, and statistical model evaluation. Third, as a proof-of-concept, the proposed methodology is applied to and validated on two distinct publicly available charging

https://doi.org/10.3390/wevj17120620

datasets, representing a residential charging station in Trondheim, Norway [23], and a public charging station in Palo Alto, California, USA [24].

Due to the limited availability of suitable publicly accessible charging datasets, these two datasets were selected to demonstrate the applicability and robustness of the proposed methodology across different charging environments. Although the selected datasets cannot be considered representative of charging stations worldwide, the primary contribution of this study lies in the proposed methodology rather than the development of universally applicable charging station utilization profiles. Given the regional and site-specific differences in charging infrastructure, driving habits, and charging behavior, accurate representation of individual charging stations requires calibration using corresponding historical data. Nevertheless, the proposed methodology remains applicable to charging stations in other geographical regions without modifications to its underlying structure, provided that suitable site-specific charging data are available for model construction and validation.

The rest of the paper is organized as follows. Section 2 defines the charging station dataset preparation, describing both the residential and public charging station datasets used as proof of concept. Section 3 presents the methodology utilized for data generation in the charging station utilization model, including the identification of optimal probability distributions for both dataset types. Section 4 defines the construction of the charging station utilization model. Section 5 discusses the comparison between input data and data generated from the presented models for both charging station types, and Section 6 concludes the paper.

2. Charging Station Dataset Preparation

The charging station utilization model enables precise modeling and representation of real-world charging station operation, reflecting the charging behavior of electric vehicle owners. The concept for the construction of the charging station utilization model presented in this paper is based on the utilization of historical charging datasets containing information about the connections and disconnections of EVs to and from the charging station, the duration of the charging sessions, and other related data. Based on the dataset used for the construction of the charging station utilization model, it is possible to represent the utilization of various types of charging stations (residential, public, workplace) or even stations providing different levels of charging (Level 2—AC fast charging, Level 3—DC charging). However, accessing datasets suitable for constructing the charging station utilization models can be challenging due to the relative scarcity and limited public availability of relevant EV charging data.

Two publicly available historical charging datasets were used to demonstrate the workflow. The residential dataset was collected at apartment buildings in Trondheim, Norway [23], over approximately December 2018–January 2020. It reports 6878 charging events involving 97 EVs over the complete recorded period. Figure 1 shows substantially fewer recorded events in the earlier months than in the later months. The published records alone do not identify the cause: changes in participation, vehicle uptake, station availability, data coverage, or other local circumstances could all contribute. The apparent increase should therefore not be attributed to EV adoption without independent supporting information.

For the proof-of-concept calibration, the residential analysis uses the comparatively active period from 15 July 2019 to 31 January 2020. The earlier records are not treated as erroneous; they are excluded to describe a selected operating regime rather than the full time-varying evolution of demand. Consequently, the calibrated distributions should not be extrapolated as a forecast of long-term EV adoption. Figure 1 displays the changes in recorded event frequency across the full original period.

https://doi.org/10.3390/wevj17120620

For the selected calibration period, a total of 5356 residential charging sessions were retained for model construction. The observation period comprised 145 workdays and 56 weekend days, which were used to estimate the time-dependent connection rates for the corresponding day types. For each of the 96 daily 15-min intervals, the connection rates were estimated from the recorded connection counts across the observed days of the respective category, including intervals with no recorded connection events. To provide further information on the availability of historical observations used for estimating connection durations, Table A1 in Appendix A reports the number of retained connection-duration observations associated with each of the 96 daily 15-min connection-start intervals, separately for workdays and weekends. These counts correspond to the observations used to construct the empirical duration distributions described in Section 2.2.

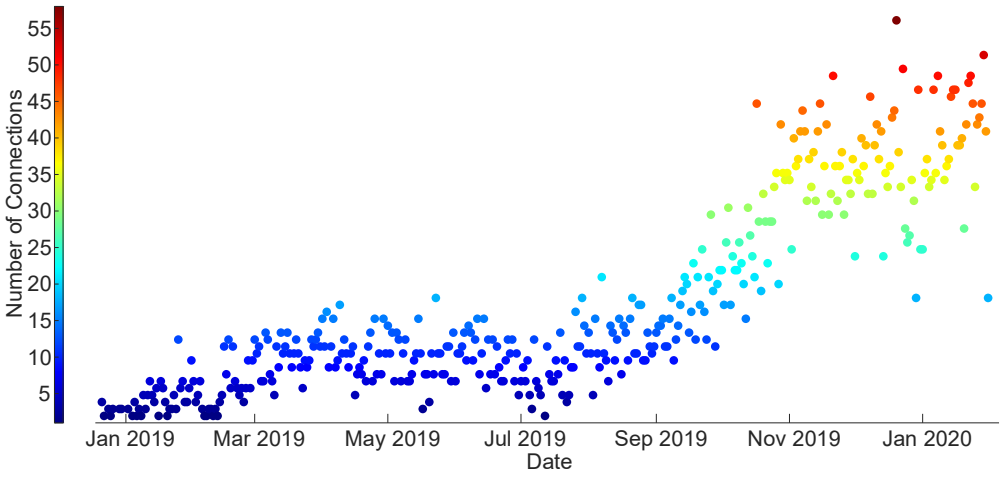


Figure 1. Frequency of charging events in the residential charging station dataset over the recorded period.

The second publicly available dataset used for the modeling of the charging station utilization model was a dataset of public charging collected from the nine publicly available charging stations distributed across the city of Palo Alto, California, USA [24]. This dataset covers a period of 113 months and 29 days, from July 2011 to December 2020, with 259,415 recorded charging events. However, similar to the residential dataset, the frequency of charging events recorded in the dataset is inconsistent. Therefore, only data recorded from January 2016 to January 2020 will be used to represent the public EVCS. The selected period was chosen based on the high frequency of charging events over this period, as shown in Figure 2. Moreover, only data from the EVCS located on Cambridge Street in Palo Alto will be used for the EVCS utilization model. This decision was made as most of the data from this EVCS was collected during the selected period. The Cambridge Street EVCS dataset contains data from 14 January 2016 to 31 December 2020, with 32,879 recorded charging events, making it one of the largest datasets in the Palo Alto collection. The frequency of charging events over the recorded period is shown in Figure 3.

The underlying reasons for the observed changes in charging event frequency cannot be conclusively determined, as the publicly available datasets do not provide sufficient contextual information to explain these variations. To characterize a specific operating regime exhibiting comparatively high and consistent charging activity, the analysis was restricted to the corresponding periods with the available historical datasets. The selection of periods exhibiting comparatively high and consistent charging activity was intended

to characterize a specific operating regime within the available historical records. The selected periods are not assumed to represent future charging behavior, and the resulting models should not be interpreted as forecasts of charging demand. Changes in station utilization resulting from evolving user behavior or charging infrastructure would require recalibration using representative historical data. Consequently, the proposed models primarily represent charging station utilization patterns observed during the selected periods rather than long-term changes in charging demand.

To provide further information on the availability of historical observations used for estimating connection durations, Table A2 in Appendix A reports the number of retained connection-duration observations associated with each of the 96 daily 15-min connection-start intervals, separately for workdays and weekends. These counts correspond to the observations used to construct the empirical duration distributions described in Section 2.2.

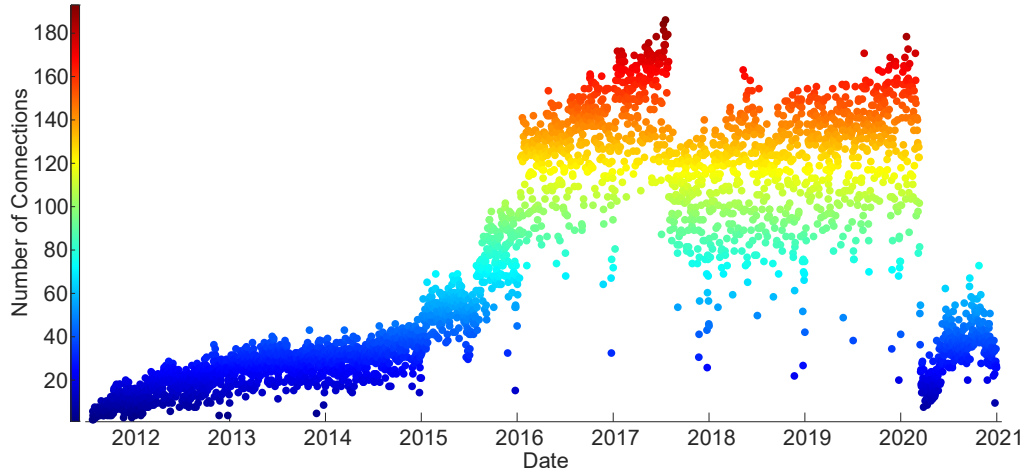


Figure 2. Frequency of charging events in the public EVCS dataset over the recorded period.

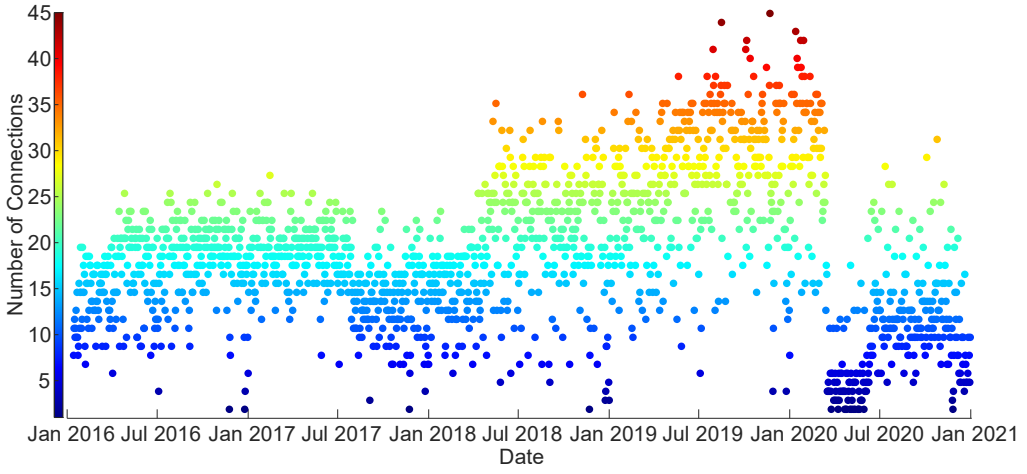


Figure 3. Frequency of charging events recorded in the EVCS on Cambridge Street over the recorded period.

To model charging station utilization, it is necessary to identify and prepare the key parameters that represent EV owners' charging habits. The main parameters used in the model presented in this paper are:

- The time of EV connection to the charging station (when);
- The duration of EV connection to the charging station (how long).

The selected parameters describe the timing of plug-in events and the length of physical connection to a charging point. Data preparation has two stages, summarized in Figure 4. First, a selected observation period is filtered, edited, and separated into workdays and weekends. Second, connection-count and duration matrices are constructed for each day type. In a 15-min representation, there are 96 clock-time bins per complete day; a bin corresponds to a start-time interval, not necessarily to 15 min of active battery charging. This workflow can be re-applied to another dataset containing sufficiently precise connection and disconnection timestamps.



Figure 4. Flowchart of data preparation for the charging station utilization model.

The first stage of data preparation is divided into three steps. In the first step, only the data corresponding to the period with the highest number of EV charging events is selected from the input datasets. In the next step, the data from the chosen period is edited into a format that can be used to construct the utilization model. In the last step of the first stage, the data from the edited datasets is divided based on the type of day (workdays, weekends). By dividing the datasets based on the day type, it will be possible to use the constructed model to represent differences in charging station utilization over a longer simulation period. Public holidays occurring from Monday to Friday (i.e., during weekdays) were classified as ordinary workdays. Holiday-specific charging behavior was not modeled separately, which represents a limitation of the proposed methodology.

The second stage of the data preparation involves further processing of the edited and divided datasets from the first stage into matrices. These matrices will contain information about the number of connections and the duration of connections to the charging station during the measured period, for both workdays and weekends. The construction of the matrices is an integral part of the data preparation process, as they will be used to construct the utilization model and represent the charging station utilization. Compiling the matrices representing the number of connections and the duration of

connections is done separately for the workday and weekend data and consists of several steps. The flowcharts illustrating the steps of the matrix's construction is shown later in Figures 5.

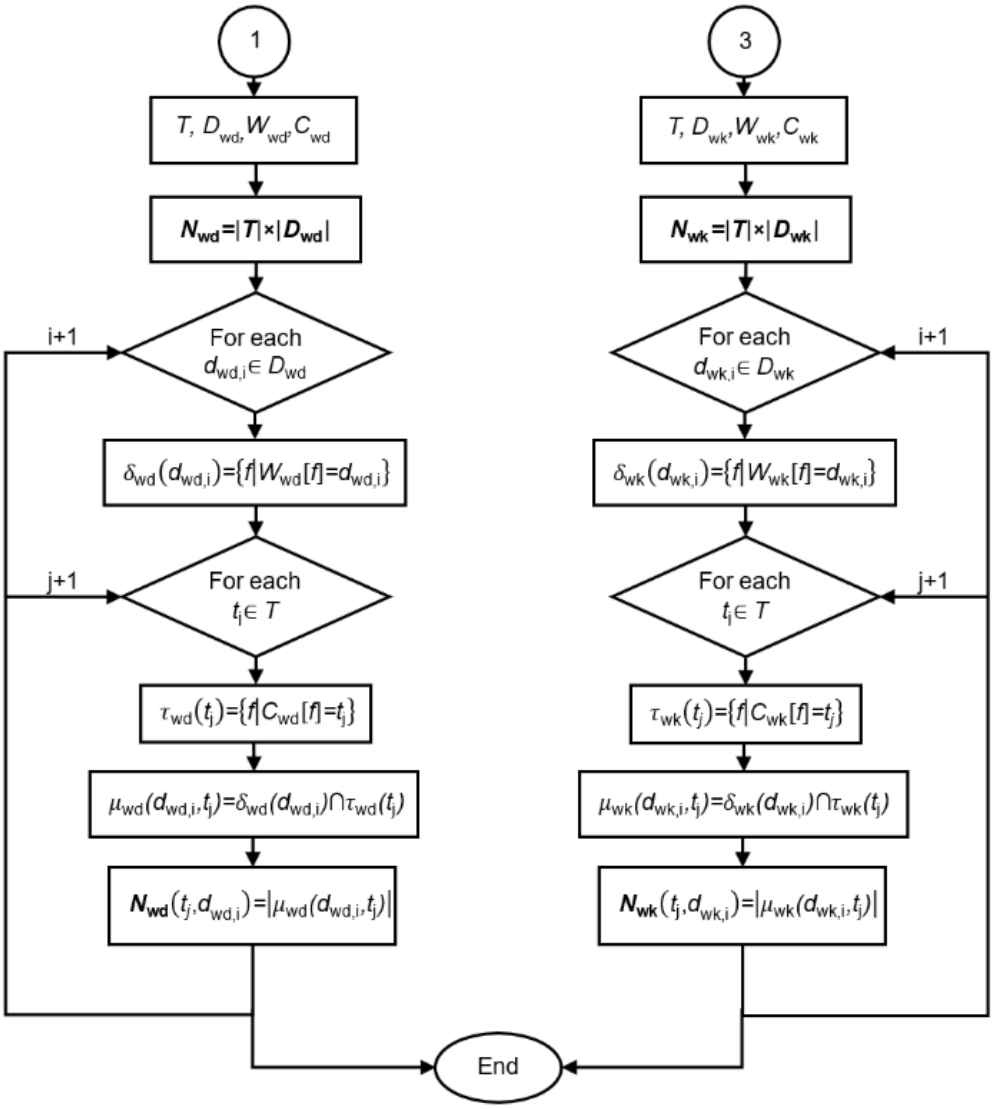


Figure 5. Flowchart illustrating the compilation process for the matrices containing information about the number of connections.

2.1. Construction of the Matrix Containing Information About the Number of Connections to a Charging Station

The matrix containing information about the number of connections to the charging station during the selected period is compiled following the flowchart illustrated in Figure 5. As can be seen from the flowchart, the matrix compilation process is identical for both workdays and weekends. Therefore, only the process corresponding to the matrix construction of the number of connections during workdays will be further explained.

The first steps in the matrix compilation process involve defining a set of vectors containing the values needed for calculating the number of connections and initializing the matrix in which the calculation results will be assigned. The vectors defined for the calculation are:

- The time vector (T);
- The vector of workday dates during the selected period (D_{wd});
- The vector of all connection dates during the workdays in the selected period (W_{wd});
- The vector of all connection times during the workdays in the selected period (C_{wd}).

Let T be the 96-element vector of quarter-hour start times in a day, and let D_{wd} be the ordered set of observed workday dates. The connection-count matrix is initialized with one row per time bin and one column per observed day, with all cells initially set to zero, using the MATLAB R2024a built-in function (*zeros*):

$$\mathbf{N_{wd}} = zeros(|T|, |D_{wd}|). \quad (1)$$

In Equation (1), *zeros* denotes a matrix filled with zero counts; its dimensions are $|T| \times |D_{wd}|$, where $T = 96$. Thus, intervals containing no recorded start events are retained as zeros rather than omitted. The same initialization is used for the weekend matrix, with the corresponding weekend date vector.

The next steps of the matrix compilation process involve calculating the number of connections to the charging station. The aim of the calculation process is to determine the number of connections in each 15-min period of a day during the selected period from the edited dataset.

During the calculation process, for each date (d_{wd}) from vector D_{wd}, we define vector δ_{wd} as the set of logical values representing matches between the date d_{wd} and the dates in vector W_{wd}. The definition of the vector δ_{wd} is then expressed as follows:

$$\delta_{wd}(d_{wd,i}) = \{j \mid W_{wd}[j] = d_{wd,i}\}. \quad (2)$$

Similarly, we define vector τ_{wd} as a set of logical values representing matches between each time $t \in T$ and the connection times in vector C_{wd}. The match vector τ_{wd} is then defined as follows:

$$\tau_{wd}(t) = \{j \mid C_{wd}[j] = t\}. \quad (3)$$

Based on the vectors δ_{wd} and τ_{wd}, we can define vector μ_{wd} as the intersection of values matching both the date d_{wd} and the time t by the following equation:

$$\mu_{wd}(d_{wd,i}, t(j)) = \delta_{wd}(d_{wd,i}) \cap \tau_{wd}(t(j)). \quad (4)$$

The last step in the matrix compilation process is to count the number of matching rows (number of connections) for each time t and each date d_{wd}. The counted connections are then written to the connection matrix at the appropriate location. This step can be expressed as follows:

$$\mathbf{N_{wd}}(t(j), d_{wd,i}) = |\mu_{wd}(d_{wd,i}, t(j))|. \quad (5)$$

The calculation process is then repeated for each date d_{wd} in the vector D_{wd}. The resulting matrix will contain information about the number of connections during the selected period in each 15-min interval of a day. An example of what the constructed matrix can look like is visualized in Figure 6. This matrix can then be used to dynamically model the representation of EVs connecting to the charging station over the course of the day and subsequently during the simulation period.

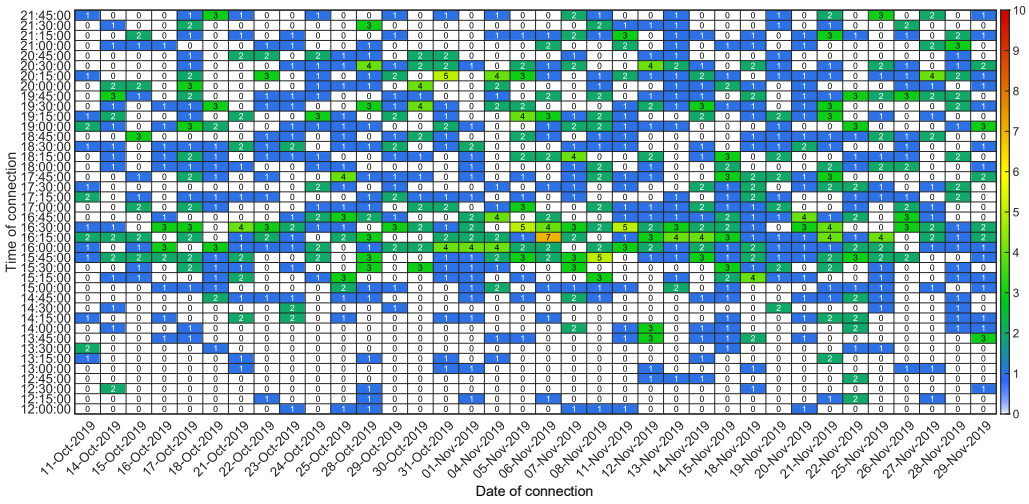


Figure 6. Representation of the number of connections matrix constructed from the source dataset for workdays.

2.2. Construction of the Matrix Containing Information About the Duration of Connections to a Charging Station

The construction process for the matrix containing information about the duration of connections during the selected period follows the flowchart illustrated in Figure 7. As can be seen from the flowchart, the matrix compilation process is identical for both workdays and weekends. Therefore, similar to the previous matrix construction, only the process corresponding to the matrix construction of the duration of connections during workdays will be further explained.

As in the previous matrix construction, the first steps involve defining a set of vectors containing the values necessary for the construction of the duration matrix. The constructed matrix will contain the distribution of the EVs' connection durations during the selected period over a day in 15-min intervals. The vectors defined for the construction of the duration matrix are:

- The time vector (T);
- The vector of connection duration times during the workdays in the selected period (K_{wd});
- The vector of all connection duration times during the workdays in the selected period (L_{wd});
- The vector of all connection times during the workdays in the selected period (C_{wd}).

The time vector T and connection-time vector C_{wd} are the same as those used for the connection matrix. Unlike the fixed-size count matrix, the duration matrix $\boldsymbol{H}_{\mathbf{wd}}$ stores historical plugged-in durations grouped according to their start-time bin and can be expanded as records are assigned. Equation (6) indicates that it is initially empty. The number of historical connection durations available for individual 15-min intervals may vary depending on the recorded charging activity. For each interval and day type, the empirical duration distribution was constructed using the available observations without combining data from neighboring time intervals or from the other day category. Consequently, distributions corresponding to intervals with relatively few recorded sessions may be more sensitive to individual observations, potentially affecting the statistical reliability of the generated connection durations. This limitation should be considered when applying the proposed methodology to datasets with sparse charging activity.

$$\boldsymbol{H}_{\mathbf{wd}} = [\,]. \tag{6}$$

https://doi.org/10.3390/wevj17120620

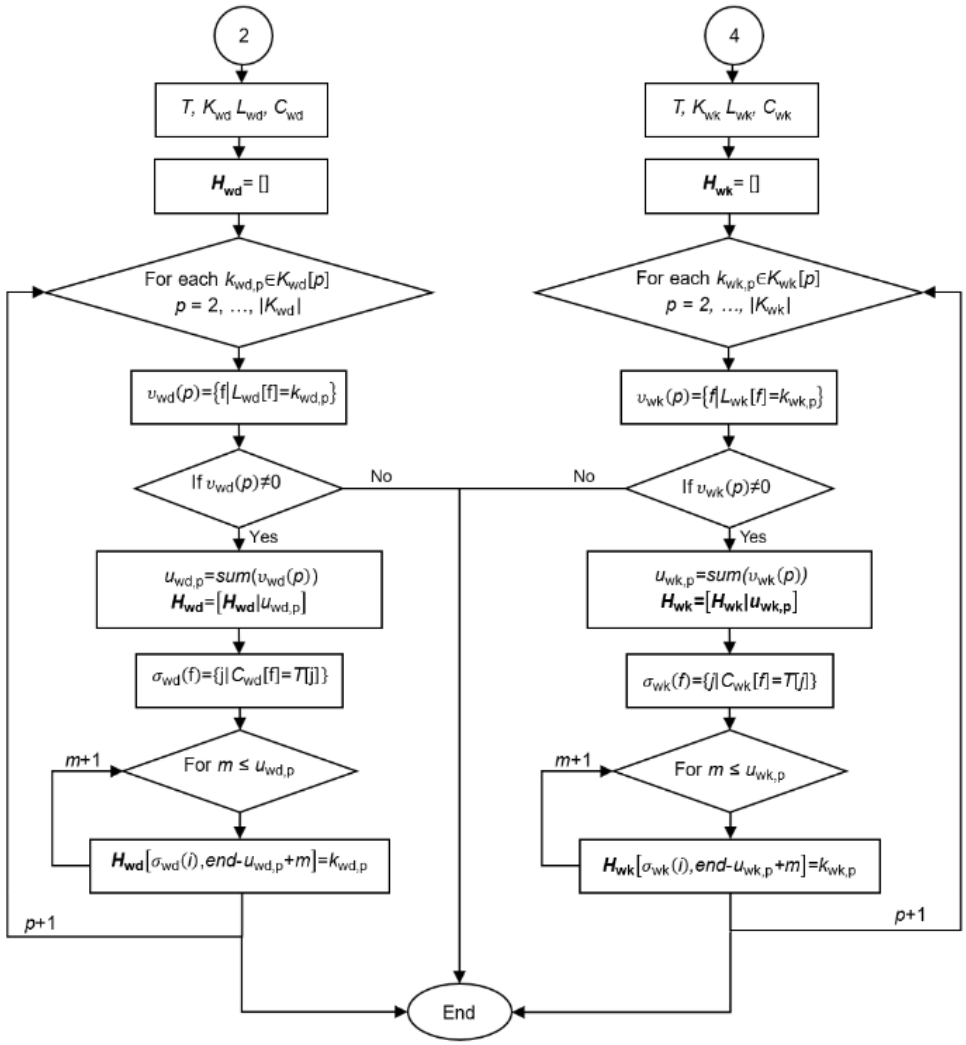


Figure 7. Flowchart illustrating the compilation process for the matrices containing information about the duration of connections.

The next step of the duration matrix construction involves gradually determining the frequency of individual connection duration times (k_{wd}) from the vector of connection duration times (K_{wd}) among all connection durations (L_{wd}) within the 15-min resolution of a day. To determine the frequency of the individual duration times over the selected period from the edited dataset, we define the vector υ_{wd} as the set of logical values representing the matches between the duration time k_{wd} and the duration times within the vector L_{wd}. The vector υ_{wd} can then be expressed as follows:

$$\upsilon_{wd}(p) = \{i | L_{wd}[i] = k_{wd,p}\}. \quad (7)$$

After determining if the duration time k_{wd} in position p has matches in vector L_{wd}, the process of determining the connection duration times frequency continues by expanding and populating the duration matrix $\boldsymbol{H}_{wd}$. The duration matrix is expanded based on the number of matches (u_{wd}) in vector υ_{wd}. The number of matches is determined by the simple sum of logical values within the vector. To populate the duration matrix, we also need to determine the corresponding 15-min period of the day (σ_{wd}) in which the EV was connected to the charging station when the corresponding connection duration was recorded. This can be expressed by the following equation:

$$\sigma_{wd}(i) = \{j | C_{wd}[i] = T[j]\}. \quad (8)$$

Based on the number of occurrences of duration time k_{wd} in vector L_{wd} and their frequency over the 15-min periods of time vector T representing one day, we can expand and populate the duration matrix. The assignment of the duration value to the corresponding position in the duration matrix $\boldsymbol{H}_{wd}$ can be expressed as follows:

$$\boldsymbol{H}_{\mathbf{wd}} = \left[\sigma_{\mathrm{wd}}(i), end - \text{-}u_{\mathrm{wd,p}} + m\right] = k_{\mathrm{wd,p}}; m = 1, \ldots, u_{\mathrm{wd,p}}. \quad (9)$$

The process of determining the distribution of individual connection duration times is repeated for every value in vector K_{wd}. The resulting matrix will contain information about the precise frequency of individual connection duration times within the selected period from the edited dataset at 15-min resolution. An example of the matrix representing the duration of the connections is illustrated in Figure 8. This matrix can then be used to dynamically model the representation of EVs being connected to the station throughout the day and subsequently during the simulation period. Moreover, with knowledge of EV connection durations to the charging station, the proposed charging station utilization model can be used to test charging control algorithms, with greater consideration of real charging station utilization.

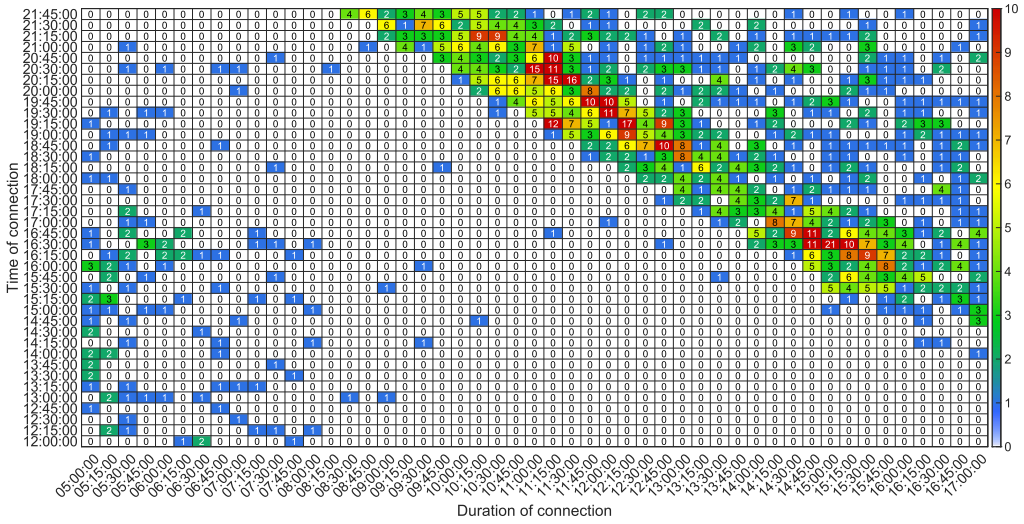


Figure 8. Representation of the duration of connections matrix constructed from source dataset for workdays.

3. Methodology of Data Generation for Charging Station Utilization Model

Before utilizing the matrices constructed to represent the utilization of the charging station for data generation, it is essential to establish the methodology that will be used for data generation. The charging station utilization model proposed in this paper utilizes a probability distribution-based method. This approach was chosen for its straightforward ability to generate new data from the input dataset with minimal modifications, while preserving the underlying distributions of the input data, thus achieving a reasonably accurate representation of the real operation of the charging station. In addition, this method also allows for easy adaptation of different datasets to the constructed model. To construct a charging station utilization model using the probability distribution method, it is necessary to determine the distribution that best fits the input dataset. To identify the best-fitting distribution, multiple approaches can be used, including goodness-of-fit tests (such as the Chi-Square test, Kolmogorov–Smirnov (K-S) test, the Anderson–Darling (A-D) test, etc.), graphical methods (such as histograms,

quantile–quantile plot, Normal probability plot, Kernel density estimation, etc.), or statistical calculations (such as mean, mode, standard deviation, median, etc.).

This paper identifies the best-fitting distribution for the input datasets representing the number of connections and the duration of connections by comparing generated and input data. This process will be applied to the dataset and further differentiated by workday and weekend data. The two-sample Kolmogorov–Smirnov goodness-of-fit test, along with graphical methods: quantile–quantile plots and histograms, will be employed to identify the best-fitting distribution for the input datasets. The methods chosen to evaluate the best-fitting distribution for the input datasets were selected based on their ability to evaluate and compare different datasets against each other, regardless of their data distribution.

The results of the two-sample Kolmogorov–Smirnov test indicate that the histogram-based probability distribution provides the closest agreement with the recorded connection durations for both workdays and weekends. Both tests failed to reject the null hypothesis at a significance level of $\alpha = 0.05$. In contrast, the alternative distributions exhibited larger discrepancies between the empirical cumulative distribution functions, resulting in statistically significant differences. These findings support the selection of the histogram-based probability distribution for representing connection durations within the examined calibration period. Nevertheless, failure to reject the null hypothesis should not be interpreted as evidence of statistical equivalence, and the results should be considered alongside the graphical comparisons presented in the corresponding histograms and Q–Q plots.

All simulations, computations, and data analysis presented in this paper were performed using the MATLAB R2024a software environment.

3.1. Identification of the Distribution for the Number of Connections to a Charging Station

The process of identifying the optimal distribution for generating data on the number of EVs connected to the charging station was carried out in two main stages. In the first stage, preprocessed matrices (described in Section 2.1) containing the necessary data to generate and represent the number of connections to the charging station were used. Different distributions were selected and tested based on the compatibility of selected distributions with the datasets used to generate the number of connections to the charging station. Therefore, eight different distributions were used for residential charging station data during identification, while only five distributions were tested for public charging station data. The generation of data for each selected distribution is initialized using the matrices from Section 2.1, separately for the residential and public charging datasets. The data generated representing the number of connections to the charging station is then used in the next stage. In the second stage, the data generated from the first stage are subjected to the K-S test and graphical evaluation to decide the optimal distribution for representation and generation of the number of EV connections to the charging station.

3.1.1. Distribution Fitting for the Number of Connections to the Residential Charging Station

The identification of the best-fitting distributions for generating data on the number of connections for the residential charging station dataset is conducted among eight different distributions. Seven of the selected distributions are generally known distributions (Birnbaum–Saunders, Exponential, Gamma, Half Normal, Kernel, Poisson, and Rayleigh), whereas one distribution is derived directly from a probability distribution of histograms constructed from the input dataset. The best-fitting distribution to represent the number of connections to the residential charging station is identified using the K-S

test, Q-Q plots, and histograms. To ensure an optimal selection of distributions, the identification process is conducted separately for both workday and weekend data.

Table 1 reproduces the K-S decisions, *p*-values, and D-values reported in the original residential comparison. Distributions not rejected by the test are highlighted, with the highest *p*-value shown in bold. The Poisson arrival model was retained because it generated nonnegative integer counts and showed visually reasonable agreement with the recorded marginal frequencies in the accompanying histograms and quantile plots. Its reported workday and weekend *p*-values were 0.9992 (D = 0.0521) and 0.9535 (D = 0.0729), respectively. These values should not be ranked as predictive accuracy or evidence that the Poisson process captures time dependence or overdispersion.

Table 1. Kolmogorov–Smirnov two-sample test from all distributions for the number of connections to the residential charging station.

Day Type	Distribution	h_0 at $\alpha = 0.05$	*p*	D	N_Historical	N_Generated
Workday	Birnbaum–Saunders	1	0.0013	0.271	3959	4396
	Exponential	1	$3.055 \cdot 10^{-5}$	0.333	3959	3093
	Gamma	0	0.3195	0.1354	3959	3577
	Half Normal	0	0.1748	0.1563	3959	5249
	Kernel	1	$1.606 \cdot 10^{-6}$	0.375	3959	5946
	Poisson	**0**	**0.9992**	**0.0521**	**3959**	**3988**
	Rayleigh	1	0.0263	0.208	3959	5952
	Histogram Probability	0	0.9899	0.0625	3959	3729
Weekend	Birnbaum–Saunders	1	0.0013	0.271	1397	1661
	Exponential	1	0.0013	0.271	1397	1063
	Gamma	0	0.0875	0.177	1397	1154
	Half Normal	0	0.1748	0.156	1397	1840
	Kernel	1	$5.972 \cdot 10^{-8}$	0.417	1397	2453
	Poisson	**0**	**0.9535**	**0.0729**	**1397**	**1390**
	Rayleigh	1	0.0065	0.2396	1397	2114
	Histogram Probability	0	0.8789	0.083	1397	1348

The graphical evaluation involved comparing the generated data with the input dataset using histograms and Q-Q plots. Histograms comparing the frequency of connections to the charging station during each 15-min interval throughout the day were constructed for both workdays and weekends and are shown in Figure 9 and Figure 10, respectively. Similar to the K S test results, the histograms generated using Gamma, Half Normal, Poisson, and histogram-based probability distributions most closely matched the input data for both workdays and weekends. Visual examination of the constructed histograms showed that histograms generated from the Poisson and histogram-based probability distributions most closely resembled the input data and effectively captured even less frequently occurring connection times. Between these two, the Poisson distribution generated data was closest to the input data, for both workdays and weekends.

The evaluation of the data generated from the selected distributions using the Q-Q plots, as shown in Figure 11 (workdays) and Figure 12 (weekends), was based on the visual assessment of the proximity of points (blue plus signs) to the reference line (red dashed line). The Q-Q plots for workdays, displayed in Figure 11, showed that most distributions closely followed the reference line in the lower quantiles. However, as quantiles increased, only the Gamma, Poisson, and histogram-based probability distributions maintained relative proximity to the reference line. Visual examination showed that the Poisson distribution consistently approximated the reference line most

closely in all quantiles. For weekend data (Figure 12), most distributions aligned well with the reference line across all quantiles. However, the Half Normal and Poisson distributions stood out, with the Poisson distribution providing the best overall fit.

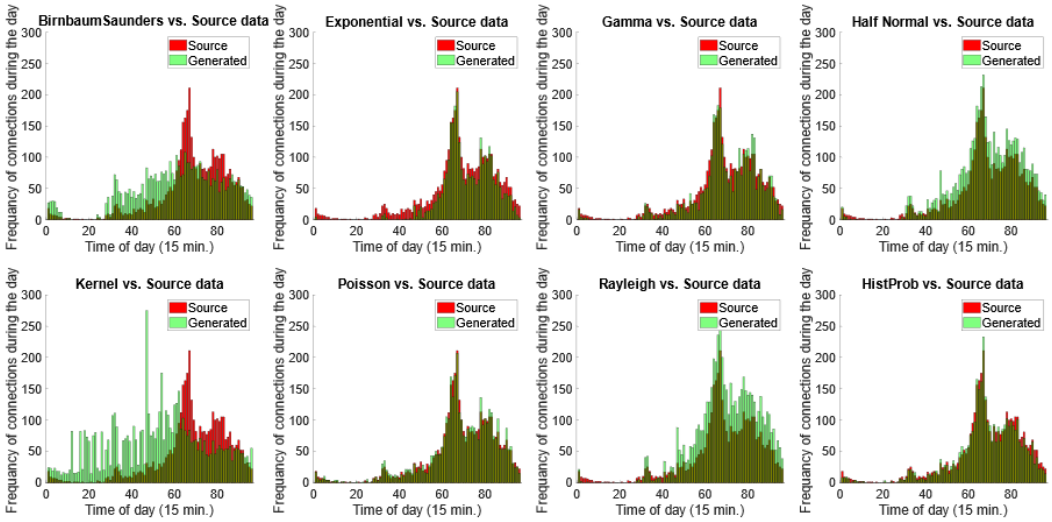


Figure 9. Histograms representing the comparison of generated data with input data for the number of connections during workdays in the residential charging station.

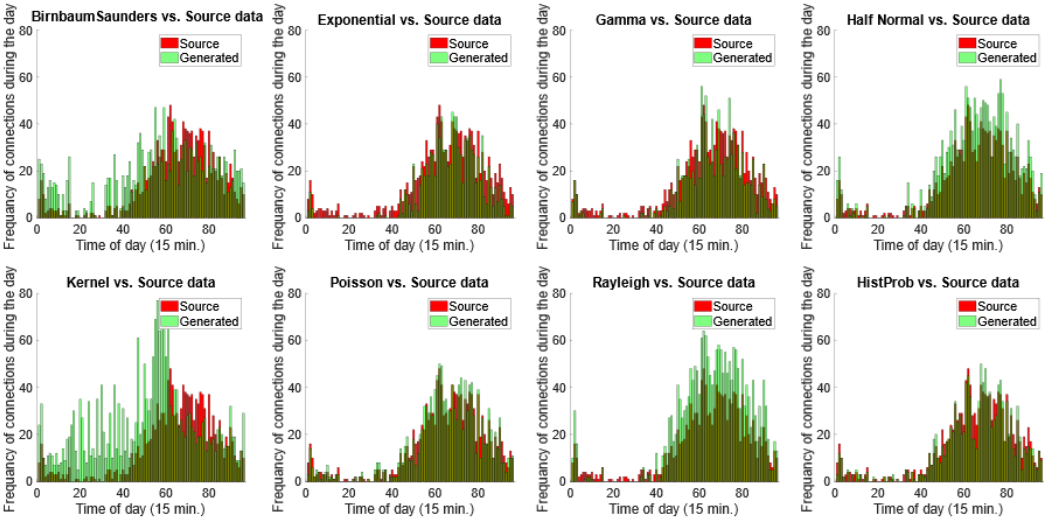


Figure 10. Histograms representing the comparison of generated data with input data for the number of connections during weekends in the residential charging station.

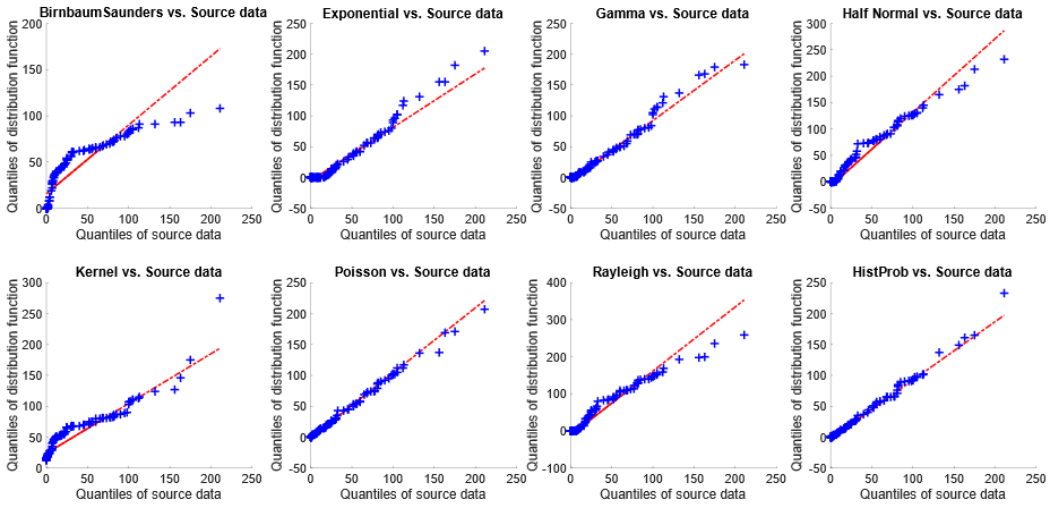


Figure 11. Q-Q plots representing the comparison of generated data with input data for the number of connections during workdays in the residential charging station.

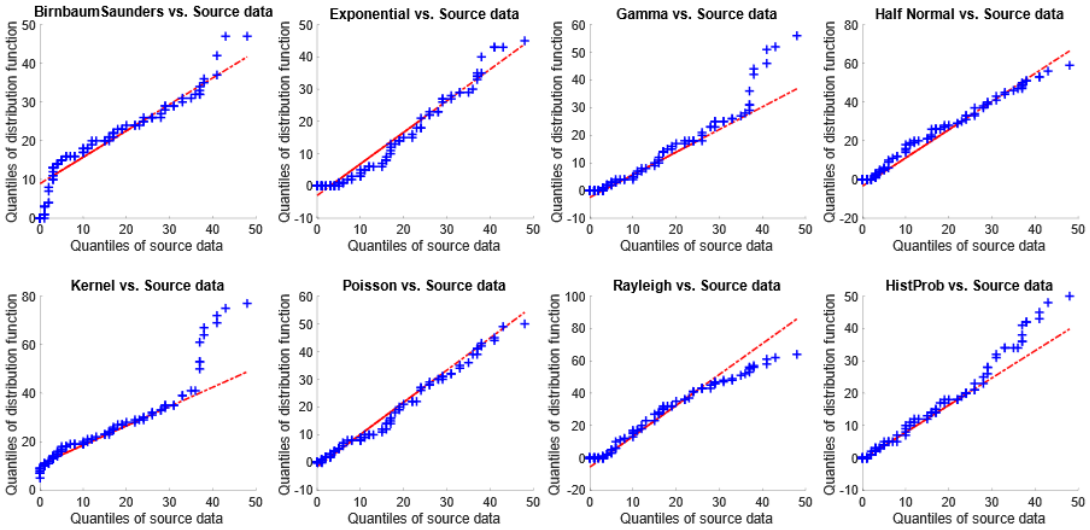


Figure 12. Q-Q plots representing the comparison of generated data with input data for the number of connections during weekends in the residential charging station.

Based on the results of the K-S test, Q-Q plots, and histograms, the Poisson distribution was selected as the most suitable to represent the number of connections to the charging station in the residential charging station utilization model, for both workdays and weekends.

3.1.2. Distribution Fitting for the Number of Connections to the Public Charging Station

The identification of the best-fitting distributions to represent the number of EV connections to the public EVCS was performed among five different distributions. These include four commonly known distributions (Half Normal, Kernel, Poisson, Rayleigh) and a custom distribution derived from the probability distribution of histograms constructed from the input dataset (Figures 13 and 14), similar to the approach used for the residential EVCS dataset. The K-S test, Q-Q plots, and histograms were employed to determine the most suitable distribution for the number of connections to the public EVCS. As with the residential EVCS, the identification process was conducted separately for workday and weekend data to ensure an optimal selection.

Table 2 presents the originally reported two-sample K-S outcomes for the public case. Poisson and empirical-histogram counts were not rejected by that test, and the Poisson

alternative was retained as a simple nonnegative integer-count model supported by the accompanying plots. The reported *p*-values of 0.9535, with D = 0.073 (workdays) and 0.9992, D = 0.0521 (weekends), are descriptive test outputs, not proof that the fitted model outperforms other arrival models or is valid out of sample.

The last evaluation of generated data was conducted using the Q-Q plots, shown in Figure 15 (workdays) and Figure 16 (weekends). From the Q-Q plots for workdays (Figure 15), it is apparent that all distributions approximate the input data up to the middle section of the reference line. Beyond this point, only the Poisson and histogram-based probability distributions remain in close proximity to the reference line. However, as observed in previous evaluations, the Poisson distribution demonstrates better results compared to the other distributions. For the weekend data (Figure 16), all selected distributions exhibit more discrepancies than in the workday case, but the Poisson distribution again provides the closest approximation to the reference line.

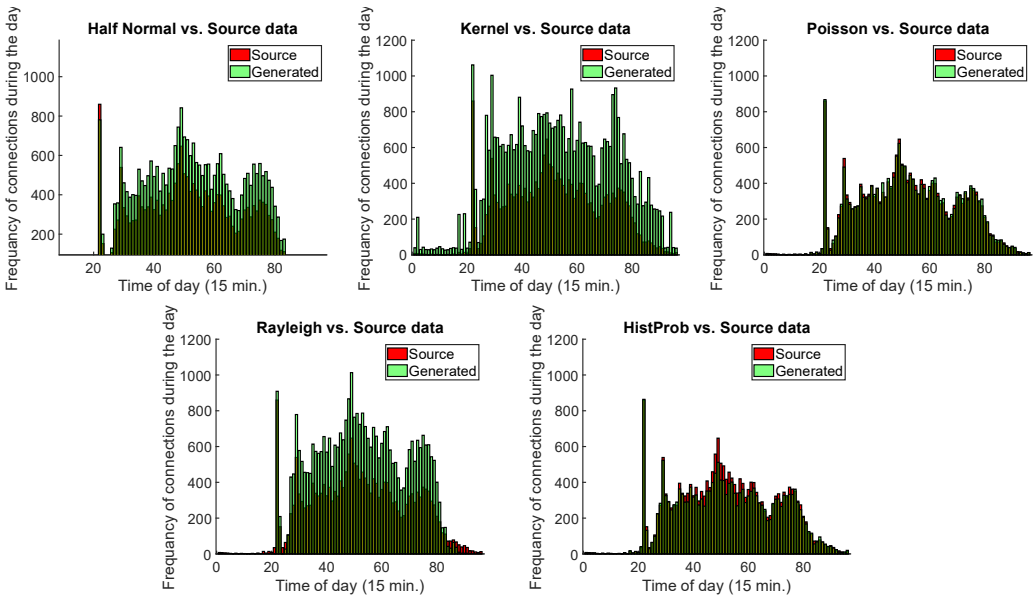


Figure 13. Histograms representing the comparison of generated data with input data for the number of connections during workdays at the public charging station.

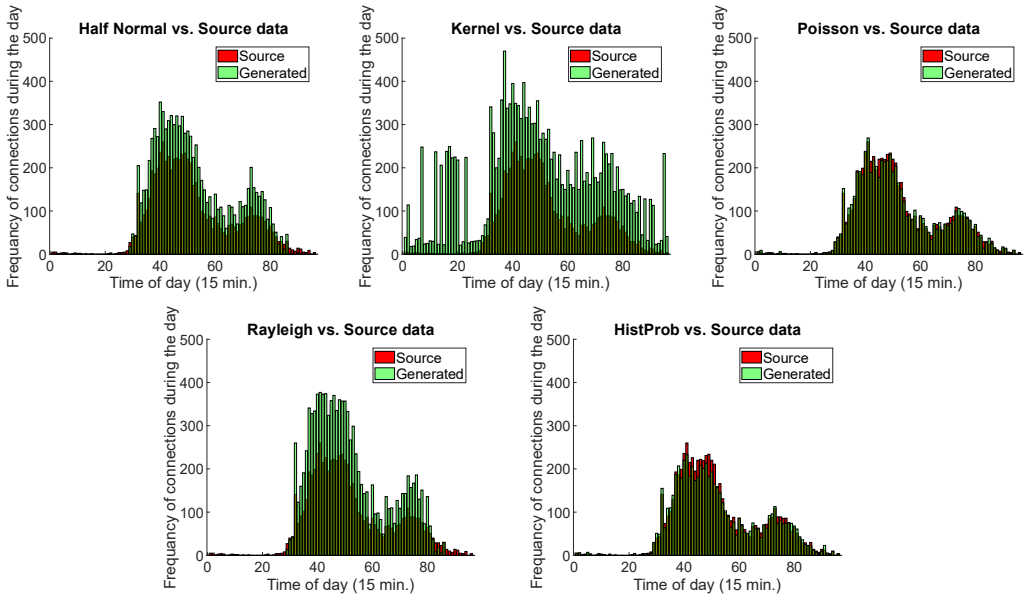


Figure 14. Histograms representing the comparison of generated data with input data for the number of connections during weekends at the public charging station.

Table 2. Results of the Kolmogorov–Smirnov two-sample test for all distributions for the number of connections to the public charging station.

Day Type	Distribution	h_0 at $\alpha = 0.05$	p	D	N_Historical	N_Generated
Workday	Half Normal	1	$1.569 \cdot 10^{-9}$	0.458	20,787	36,077
	Kernel	1	$1.170 \cdot 10^{-12}$	0.531	20,787	48,627
	Poisson	**0**	**0.9535**	**0.073**	**20,787**	**20,976**
	Rayleigh	1	$1.170 \cdot 10^{-12}$	0.531	20,787	42,101
	Histogram Probability	0	0.239	0.146	20,787	19,329
Weekend	Half Normal	1	$7.456 \cdot 10^{-4}$	0.281	6476	11,741
	Kernel	1	$1.170 \cdot 10^{-12}$	0.531	6476	19,052
	Poisson	**0**	**0.9992**	**0.0521**	**6476**	**6553**
	Rayleigh	1	$4.109 \cdot 10^{-4}$	0.292	6476	13,534
	Histogram Probability	0	0.9535	0.073	6476	6310

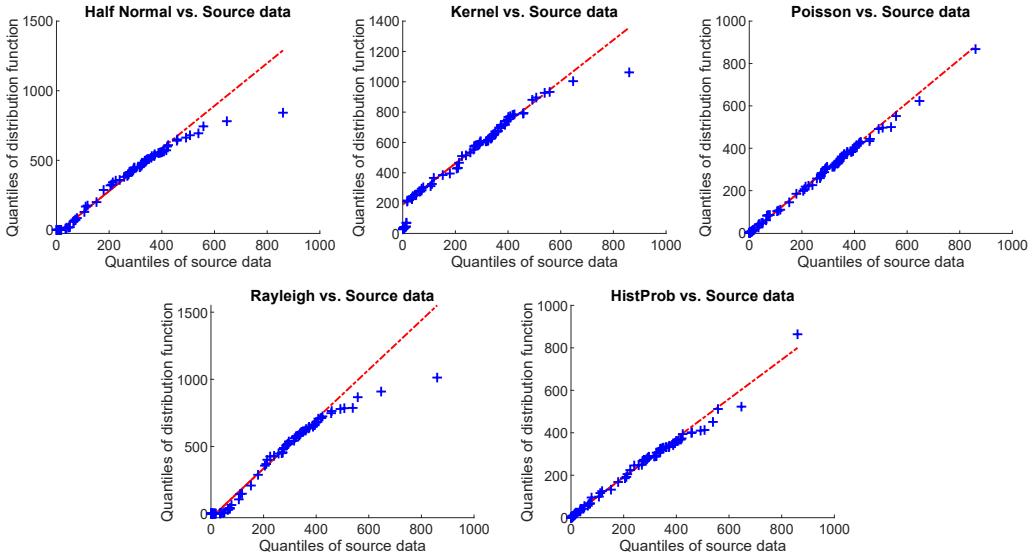


Figure 15. Q-Q plots representing the comparison of generated data with input data for the number of connections during workdays in the public charging station.

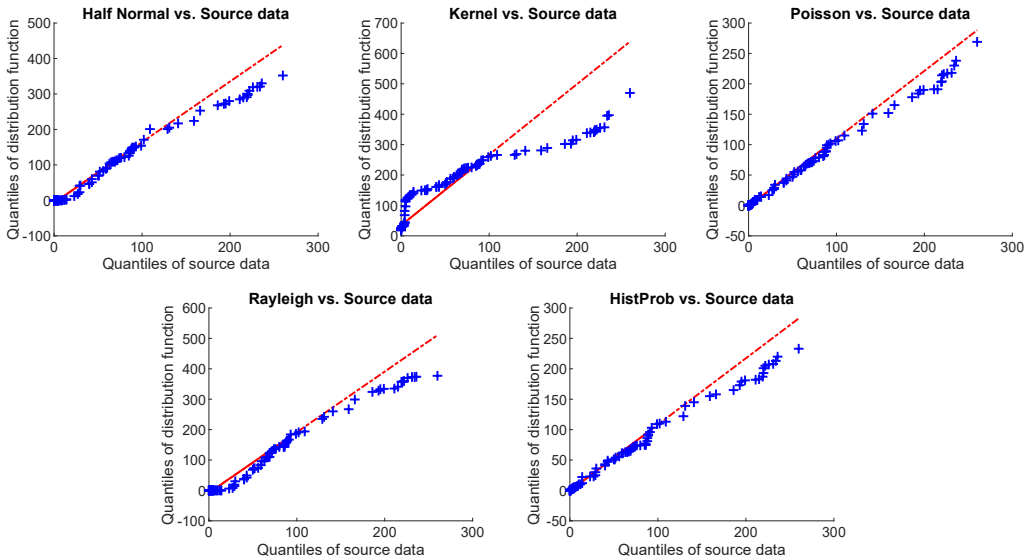


Figure 16. Q-Q plots representing the comparison of generated data with input data for the number of connections during weekends in the public charging station.

Based on the combined results from the K-S test, histograms, and Q-Q plots, the Poisson distribution was identified as the most suitable distribution to represent the number of connections to the public charging station, consistent with the results obtained for the previous dataset. This distribution has consistently produced the best results for both workday and weekend data and, therefore, can be utilized in the public charging station utilization model based on this testing.

3.2. Identification of the Distribution Functions for the Duration of Connections to a Charging Station

The process of identifying the optimal distribution for generating data on the duration of EV connections to the charging station follows the same methodology used to determine the optimal distribution for the number of connections. This process is therefore carried out similarly in two stages. In the first stage, the preprocessed matrices (described in Section 2.2) containing the necessary data to generate and represent the duration of connections to the charging station are utilized. Data generation is conducted separately for workdays and weekends, with each selected distribution being applied independently. Selected distributions were again selected based on the compatibility of the chosen distributions with the used data. The second stage focuses on evaluating the generated data to determine the optimal distribution to accurately represent the duration of EV connection to the charging station. This evaluation involves the application of the K-S two-sample test, as well as a graphical assessment using Q-Q plots and histograms. These tools will collectively help determine which distribution best fits the characteristics of the input dataset, ensuring that the generated data closely mirrors real-world observations.

3.2.1. Distribution Fitting for the Duration of Connections to the Residential Charging Station

Identifying the best-fitting distributions for generating data on the duration of EV connections to the residential charging station is conducted similarly to determining the distribution for the number of connections. The identification is considered among eight different distributions (Birnbaum–Saunders, Exponential, Gamma, Half Normal, Kernel, Poisson, Rayleigh, and histogram-based probability). The best-fitting distribution for the representation of the duration of connections is evaluated separately for workdays and weekends using the K-S test, Q-Q plots, and histograms.

Table 3 records the originally reported K-S p-values for candidate residential connection-duration models. Of the distributions tested, the empirical-histogram method was the only one not rejected for both workdays ($p = 0.5386$, D = 0.018) and weekends ($p = 0.9999$, D = 0.011). These are descriptive results on the calibration data, not formal evidence of equivalence or prediction performance.

Table 3. Results of the Kolmogorov–Smirnov two-sample test from all distributions for the duration of connections to the residential charging station.

Day Type	Distribution	h_0 at $\alpha = 0.05$	p	D	N_Historical	N_Generated
Workday	Birnbaum–Saunders	1	$5.544 \cdot 10^{-95}$	0.231	3835	4396
	Exponential	1	0	0.875	3835	3093
	Gamma	1	0	0.667	3835	3577
	Half Normal	1	0	0.591	3835	5249
	Kernel	1	$7.181 \cdot 10^{-101}$	0.222	3835	5946
	Poisson	1	0	0.809	3835	3988
	Rayleigh	1	0	0.599	3835	5952
	Histogram Probability	**0**	**0.5386**	**0.018**	**3835**	**3729**

Weekend	Birnbaum–Saunders	1	$8.82 \cdot 10^{-41}$	0.245	1378	1661
	Exponential	1	0	0.904	1378	1063
	Gamma	1	$1.194 \cdot 10^{-255}$	0.685	1378	1154
	Half Normal	1	$3.117 \cdot 10^{-237}$	0.584	1378	1840
	Kernel	1	$8.089 \cdot 10^{-51}$	0.257	1378	2453
	Poisson	1	0	0.835	1378	1390
	Rayleigh	1	$1.191 \cdot 10^{-259}$	0.597	1378	2114
	Histogram Probability	**0**	**0.9999**	**0.011**	**1378**	**1348**

Graphical evaluation using histograms shown in Figures 17 and 18 confirmed the K-S test results. A comparison between the data generated from each distribution and the input data showed that the other selected distributions struggle to adequately represent the full range of connection durations. These distributions tend to generate predominantly short connection durations or a limited combination of durations, failing to capture the diversity seen in the input dataset. In contrast, the histogram-based probability distribution successfully generates data with minimal discrepancies for both workdays and weekends.

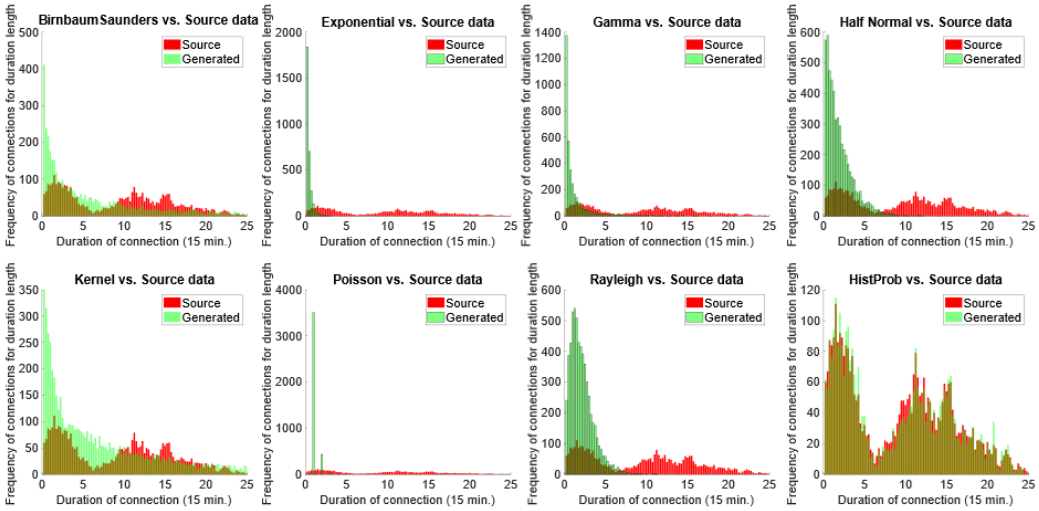


Figure 17. Histograms representing the comparison of generated data with input data for the duration of connections during workdays in the residential charging station.

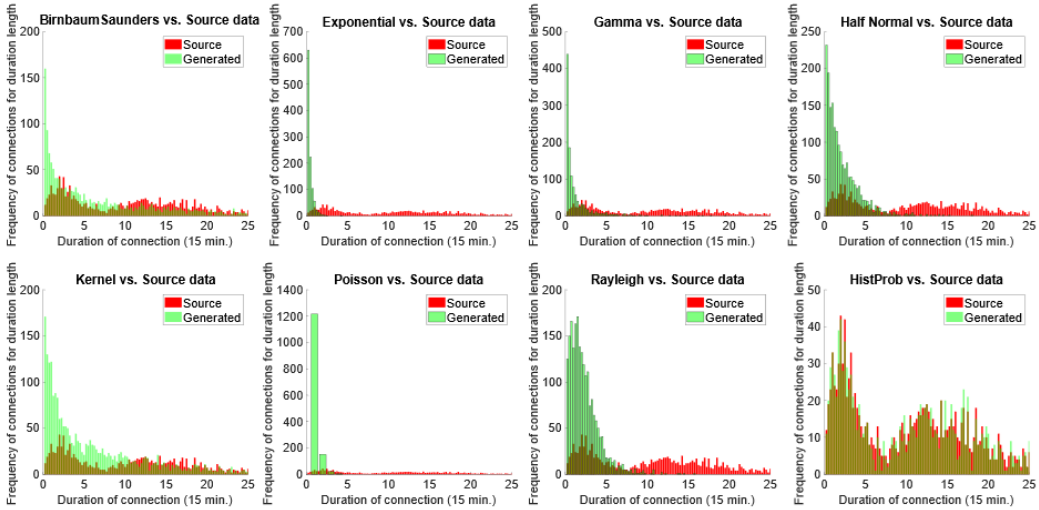


Figure 18. Histograms representing the comparison of generated data with input data for the duration of connections during weekends in the residential charging station.

The Q-Q plots (Figures 19 and 20) further supported these findings, showing that only the histogram-based distribution had points that aligned with the reference line across all quantiles, for both workday and weekend data. Given the consistent and conclusive results across all evaluation methods, the histogram-based probability distribution will be utilized to represent and generate data for EV connection durations in the residential charging station utilization model.

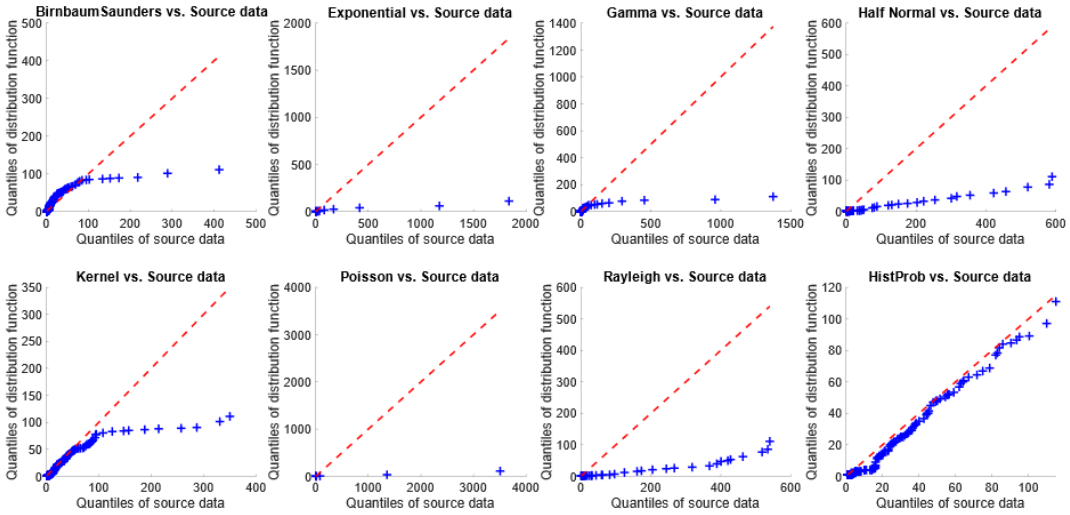


Figure 19. Q-Q plots representing the comparison of generated data with input data for the duration of connections during workdays in the residential charging station.

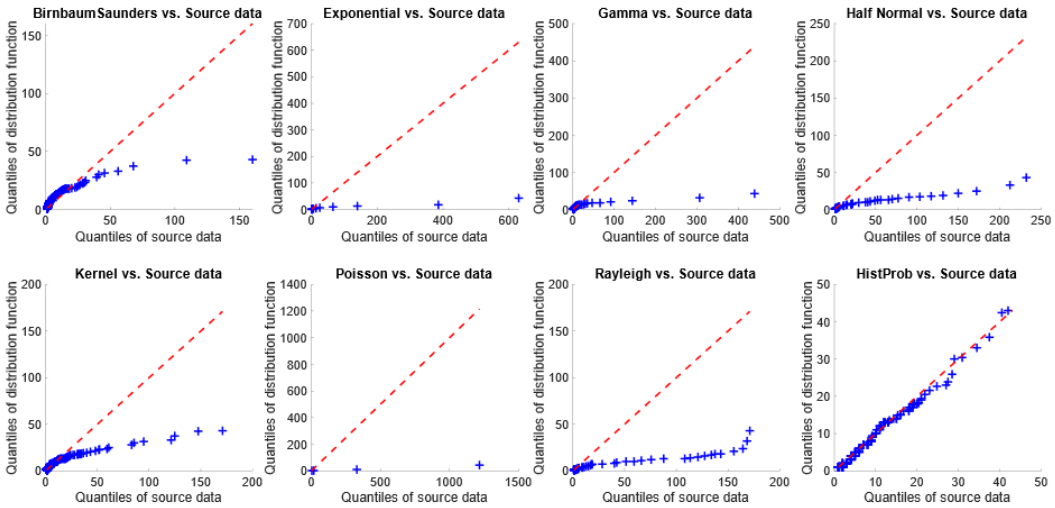


Figure 20. Q-Q plots representing the comparison of generated data with input data for the duration of connections during weekends in the residential charging station.

3.2.2. Distribution Fitting for the Duration of Connections to the Public Charging Station

The process of identifying the best-fitting distributions for the duration of EV connections to the public charging station closely mirrors the approach used for the residential charging station dataset. This evaluation was conducted for five different distributions (Half Normal, Kernel, Poisson, Rayleigh, and histogram-based probability), and separately for workday and weekend data. The selected distributions were, as in previous cases, chosen based on the characteristics of the parameters required for the construction of the public charging station utilization model.

The results of the K-S test for the duration of EV connections are presented in Table 4. The results indicate that, similar to the residential charging station case, only the

histogram-based probability distribution did not reject the null hypothesis for both workday (p = 0.8793, D = 0.0059) and weekend (p = 0.955, D = 0.0091) data.

Table 4. Results of the Kolmogorov–Smirnov two-sample test from all distributions for the duration of connections to the public EVCS.

Day Type	Distribution	h_0 at α = 0.05	p	D	N_Historical	N_Generated
Workday	Half Normal	1	0	0.822	20,787	36,077
	Kernel	1	0	0.330	20,787	48,627
	Poisson	1	0	0.751	20,787	20,976
	Rayleigh	1	0	0.840	20,787	42,101
	Histogram Probability	**0**	**0.8793**	**0.0059**	**20,787**	**19,329**
Weekend	Half Normal	1	0	0.697	6476	11,741
	Kernel	1	$9.676 \cdot 10^{-19}$	0.066	6476	19,052
	Poisson	1	0	0.489	6476	6553
	Rayleigh	1	0	0.733	6476	13,534
	Histogram Probability	**0**	**0.955**	**0.0091**	**6476**	**6310**

The histogram evaluation of the generated data is shown in Figures 21 and 22, confirming the findings from the K-S test. A comparison between the generated data from each distribution and the input data revealed that only the histogram-based probability distribution was able to generate data with minimal discrepancies for both workdays and weekends.

The evaluation of the Q-Q plots shown in Figures 23 and 24 further supports the findings from the K-S test and histogram evaluation. The Q-Q plots demonstrate that only the histogram-based probability distribution consistently displayed points in close proximity to the reference line for both workdays and weekends.

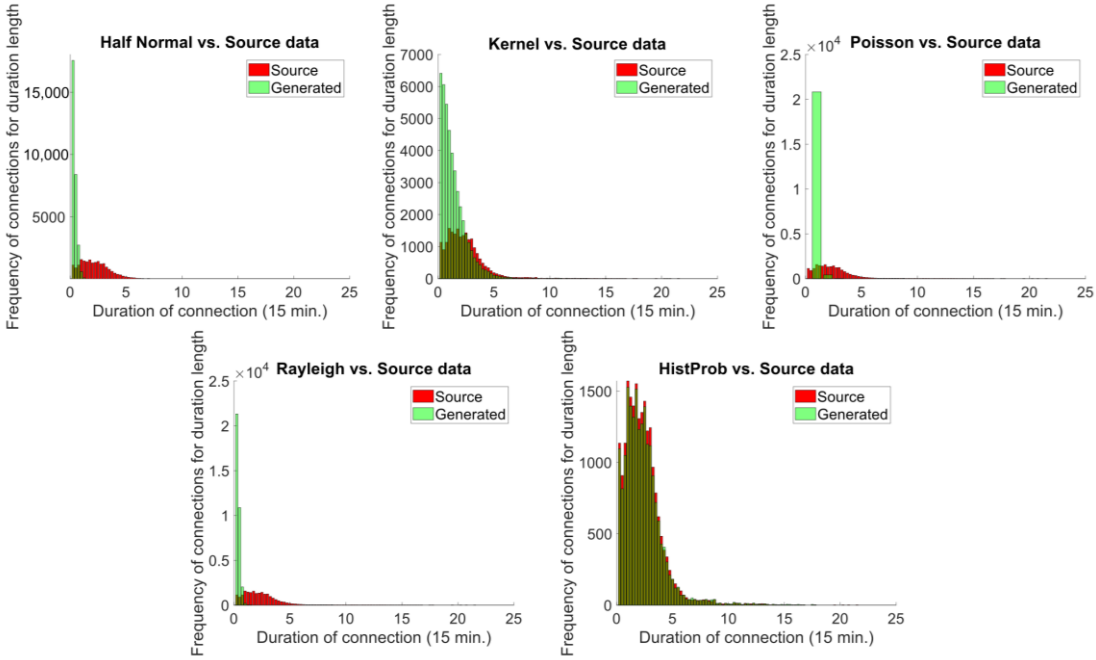


Figure 21. Histograms representing the comparison of generated data with input data for the duration of connections during workdays in the public charging station.

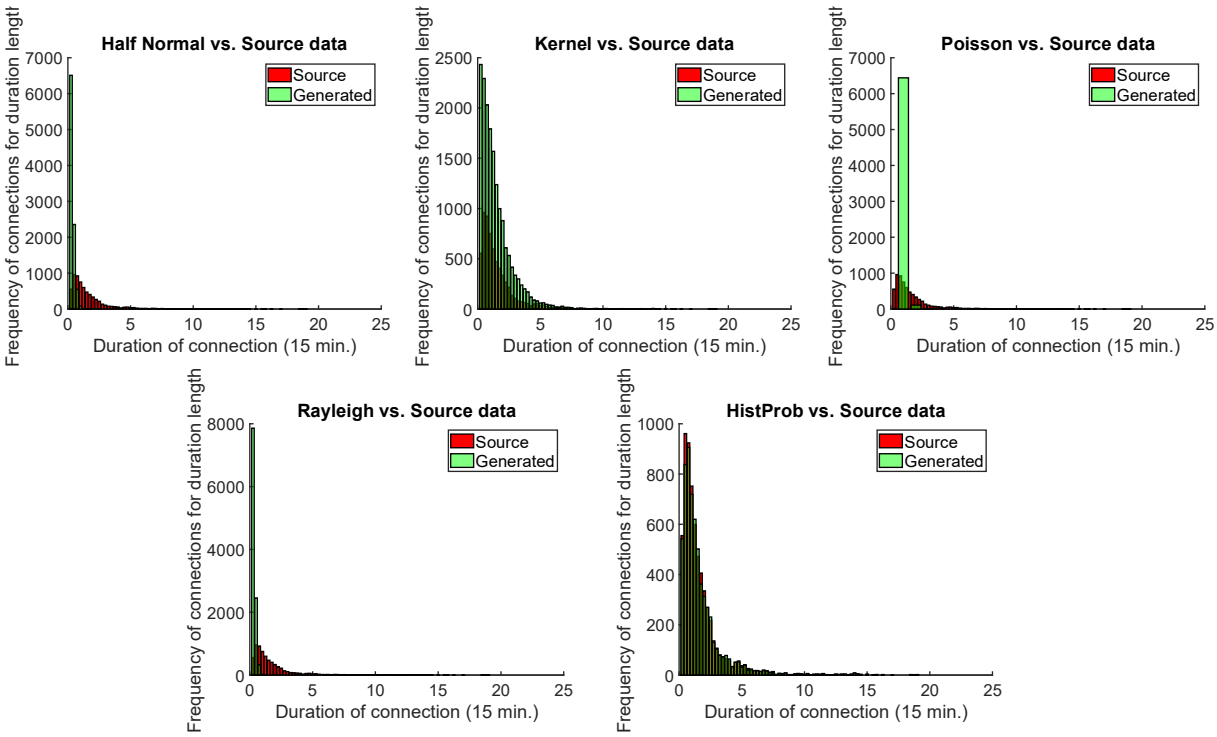


Figure 22. Histograms representing the comparison of generated data with input data for the duration of connections during weekends in the public charging station.

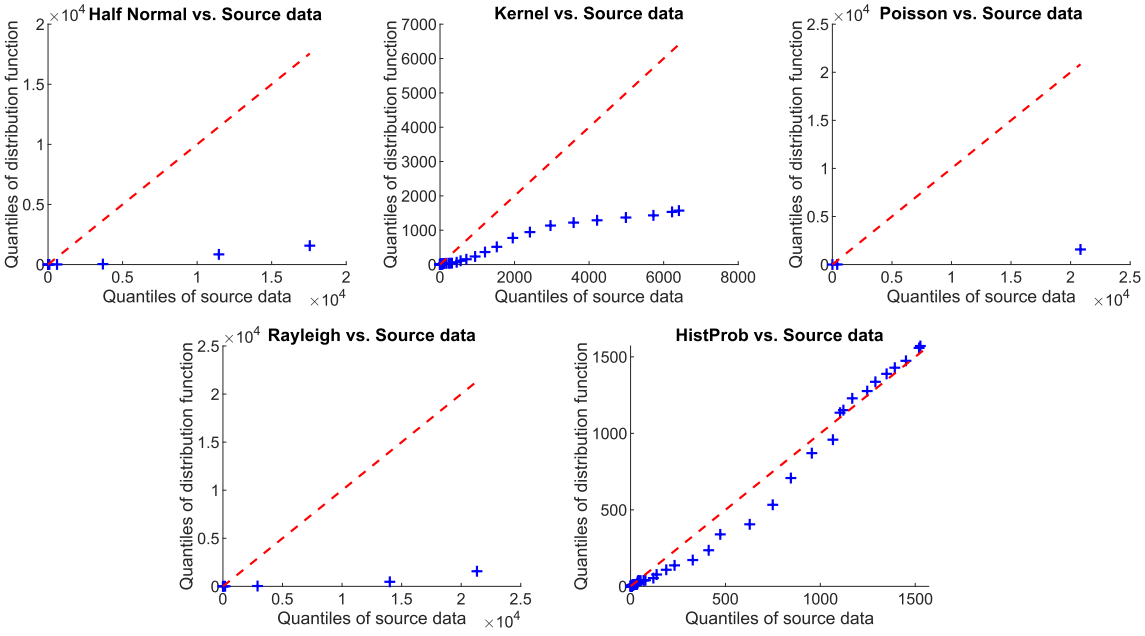


Figure 23. Q-Q plots representing the comparison of generated data with input data for the duration of connections during workdays in the public charging station.

https://doi.org/10.3390/wevj17120620

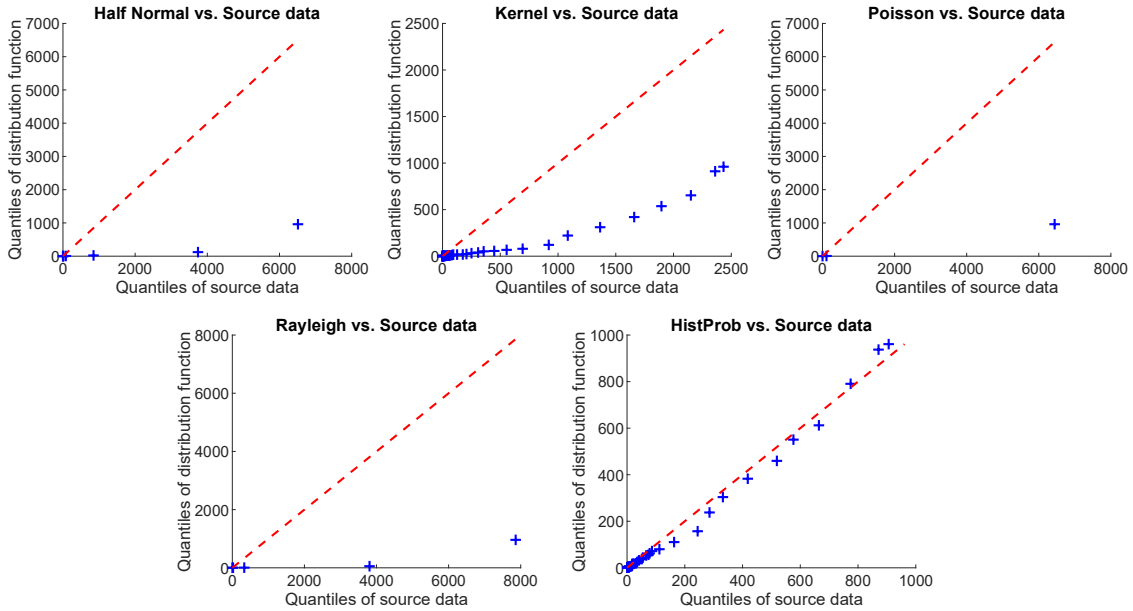


Figure 24. Q-Q plots representing the comparison of generated data with input data for the duration of connections during weekends in the public charging station.

Given the consistency of the presented results from all evaluation methods, the histogram-based probability distribution can be used to represent and generate data for EV connection durations in the public charging station utilization model.

4. Construction of the Charging Station Utilization Model

The construction of the charging station utilization model presented in this paper involves the sequential generation of data representing charging station utilization over the simulation period. To accurately model this utilization, two key parameters are defined: the number of EV connections to the charging station at each time step and the connection duration of each EV. The proposed model is designed to represent the utilization of charging stations over any arbitrary time period and for charging stations of varying sizes. This flexibility is achieved through a data generation method based on probability distributions, which represent the necessary parameters as described in the previous section, and the ability to normalize these parameters.

The construction process of the charging station utilization model is divided into four main stages, as illustrated in Figure 25.

In the first stage, the length of the simulation period (T_{sim}) is set by specifying the start (t_s) and end (t_e) dates. The size of the simulated charging station is defined by the number of charging stands (A) or the number of EVs. Additionally, during this stage, the matrices containing data necessary for generating parameters that represent charging station utilization are prepared for the construction process. Data generation is then initialized and proceeds gradually for each day (t_{sim}) within the simulation period, classifying each simulated day as either a workday or weekend. This classification is important because, as established in Section 2, the charging patterns differ between these two day types, and the matrices used for data generation are maintained separately for each. By iterating through the simulation period day by day and selecting the appropriate dataset, the model preserves the weekly rhythm of real charging station utilization throughout the entire simulated period.

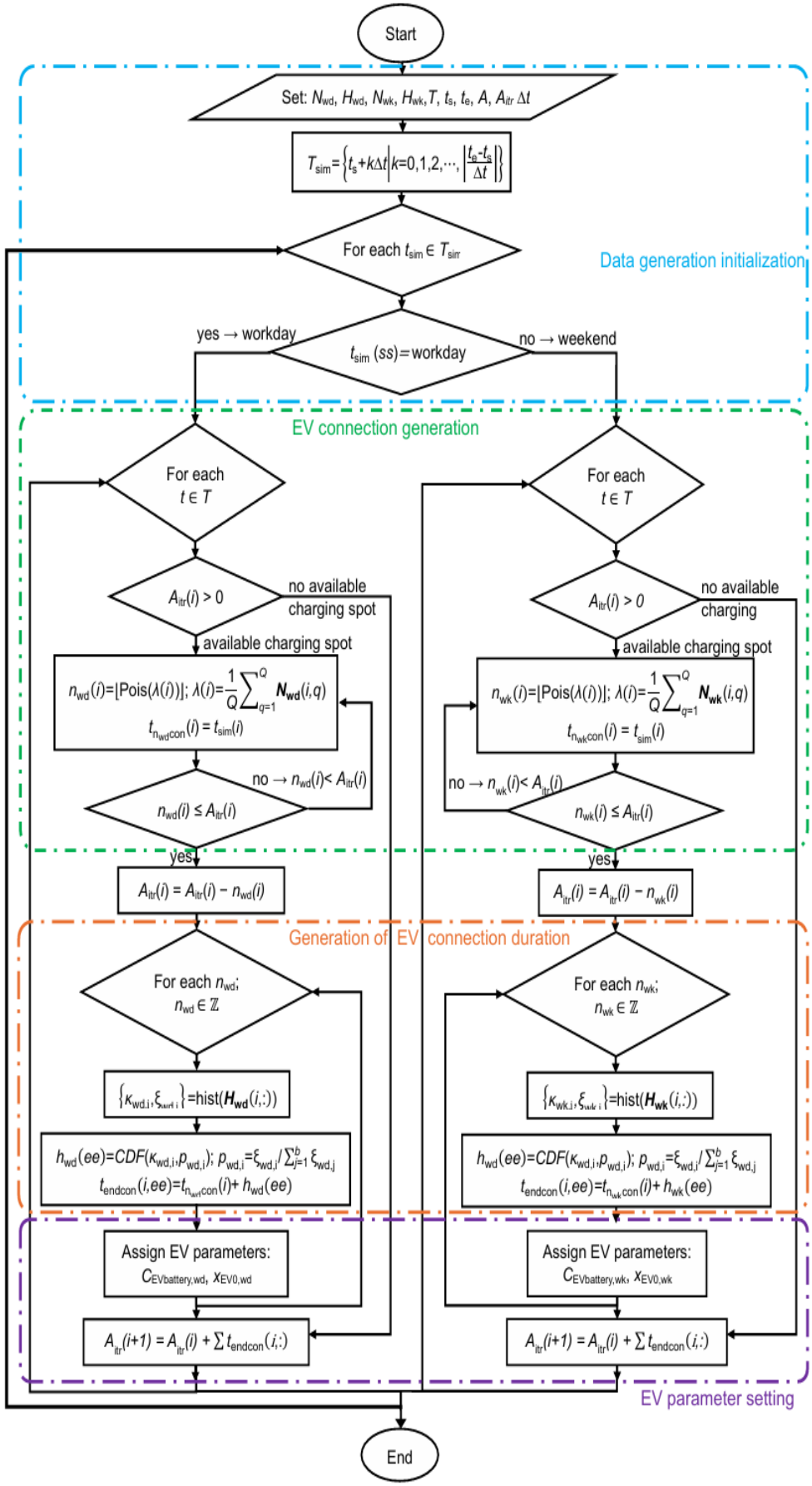


Figure 25. Flowchart illustrating the work process of the charging station utilization model.

The second stage involves generating the number of EV connections (n) to the charging station. During this process, EV connections are generated for each day in 15-min intervals (t; t = 1, 2,…i; i = 24/0.25) using the probability distribution method. At each time step i, the model draws a random value from a Poisson distribution whose rate parameter $\lambda(i)$ is computed as the average number of connections historically observed at that specific 15-min slot across all days of the same type (workday or weekend) in the dataset. Concretely, $\lambda(i)$ is the row-wise mean of the connection matrix N constructed in Section 2. This means that if, for example, EV arrivals historically peak between 18:00 and 19:00, the Poisson rate at those time steps will be higher, and the model will generate more connections during that window on average. The Poisson distribution was identified as the best-fitting distribution for this parameter in both the residential and public charging station datasets, as discussed in Section 3.1. The generation of the number of connections can be expressed as follows:

$$n_{\mathrm{wd}}(i)=\lfloor \mathrm{Pois}(\lambda(i)) \rfloor;\ \lambda(i)=\frac{1}{Q}\sum_{q=1}^{Q}\mathbf{N_{wd}}(i,q), \tag{10}$$

where $n_{\mathrm{wd}}(i)$ is the number of EV connections generated for the workday at time step i, $\lambda(i)$ is the lambda parameter of the Poisson distribution, Q is the number of days during the simulation period for the i-th time step, and $\mathbf{N_{wd}}(i,q)$ is the matrix representing the number of connections during workdays. The weekend data generation is performed similarly.

An important constraint is enforced during the connection generation step: the model tracks the number of currently available charging spaces (A_{itr}). At each time step, if the number of newly generated connections exceeds the number of free spots, the excess connections are discarded, ensuring that the total number of simultaneously connected EVs never surpasses the physical capacity of the station. The available spot count is then updated based on the connection end times computed later in Stage 3, so that spots become free again once an EV disconnects. This mechanism is what allows the model to accurately replicate the occupancy dynamics of a real charging station over time.

The recorded datasets contain only sessions that obtained a charging point; arrivals that found the station fully occupied are not observed. The estimated rates $\lambda(i)$ therefore describe accepted (served) demand, which is a lower bound of attempted demand. When the station is simulated at its historical size, the capacity constraint acts as a physical consistency safeguard rather than as a model of unserved demand. Arrivals discarded by it slightly reduce the number of generated sessions in high-occupancy periods, while the duration distribution conditional on the arrival slot is unaffected. In queueing terms, the generator is a time-inhomogeneous Erlang loss system with arrival-time-dependent empirical service times.

The third stage involves generating the duration of each individual EV connection (h) for each EV connected to the charging station. Rather than using a standard parametric distribution, the model samples directly from the empirical distribution of connection durations observed in the historical dataset. This is achieved using the duration matrix H constructed in Section 2, which stores the recorded durations indexed by the 15-min time slot in which the connection started. When generating the duration of an EV that connects at time step i, the model extracts row i of the duration matrix, constructs a histogram from the values in that row, and samples a duration value from this empirical distribution using the cumulative distribution function (CDF). This design ensures that the generated durations are statistically consistent with what was historically observed, specifically at that time of day, capturing the realistic correlation between arrival time and charging duration. For example, EVs connecting late in the evening tend to remain connected overnight and thus have longer durations, whereas vehicles arriving in the morning may charge for shorter periods. The histogram-based probability distribution was identified as

the best-fitting approach for modeling connection durations in both the residential and public charging station datasets, as discussed in Section 3. The generation process can be expressed as:

$$\{\kappa_{wd,i},\xi_{wd,i}\}=\text{hist}(\boldsymbol{H_{wd}}(i,:)), \tag{11}$$

$$h_{wd}(ee)=CDF(\kappa_{wd,i},p_{wd,i});\ p_{wd,i}=\frac{\xi_{wd,i}}{\sum_{j=1}^{b}\xi_{wd,j}},\ \text{for } i=1,2,..,b, \tag{12}$$

where $\kappa_{wd,i}$ represents the values of charging durations and $\xi_{wd,i}$ the frequencies of these values in the histogram generated from matrix $H_{wd}(i,:)$ for the i-th time step. $h_{wd}(ee)$ is the duration of the ee-th EV connected at the i-th time step during workdays, CDF is the cumulative distribution function used for values from the generated histogram, $p_{wd,i}$ is the probability of selecting the i-th value from the histogram, and b is the number of bins in the histogram. Connection durations for weekends are generated in the same manner. It is worth noting that the histogram is built fresh for each time step i and each day type, meaning the probability of drawing a particular duration dynamically adapts to the distribution of durations observed at that specific time of day in the historical data.

From the generated connection duration and the time of connection, the model computes the end time of each EV session. These end times are stored and used to update the count of available charging spots at future time steps: a spot is marked as free again only once the end time of the EV currently occupying it has passed. This mechanism links stages 2 and 3 into a coherent, physically consistent simulation of station occupancy over time. The example of what the occupancy matrix of the charging station looks like is visualized in Figure 26. From the figure, it can be observed when and how many EVs are connected to the charging station.

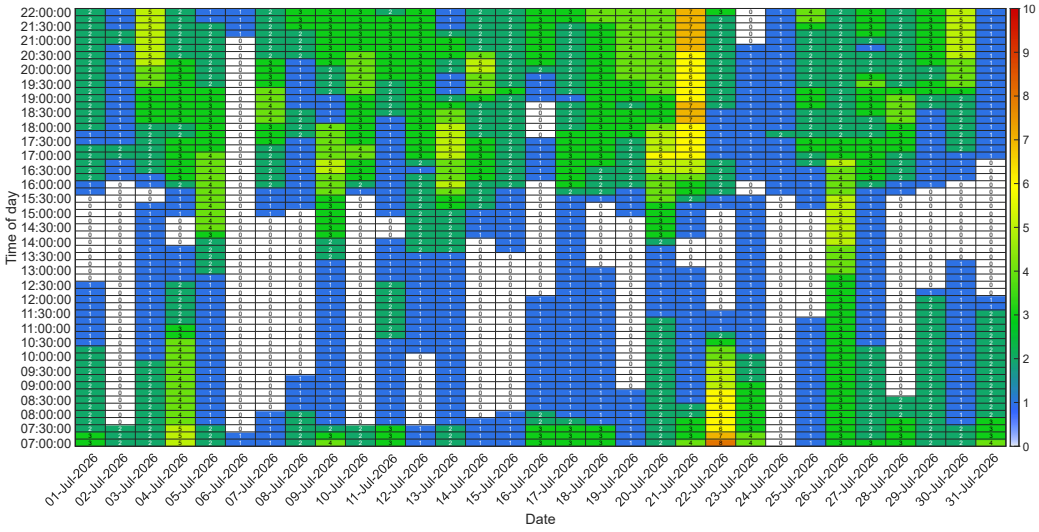


Figure 26. Representation of the generated occupancy matrix of the residential charging station for the selected period.

In the final stage, additional EV-related parameters, including battery capacity ($C_{EVbattery}$) and initial state of charge (x_{EV0}), may be assigned for potential use in subsequent charging-management studies. However, these parameters are not used to calculate or evaluate charging power or energy consumption in the present study. The evaluated outputs are the generated connection events and plugged-in connection durations, while station occupancy is constructed using the charging-point capacity constraints.

The four-stage generation process described above is repeated for every 15-minute interval of every simulated day throughout the simulation period, progressing

chronologically until the end date is reached. The resulting output is a complete time-series record of EV connections, their durations, and the associated occupancy of the charging station. Because the same construction procedure is applied identically to the residential and public charging station models, the only elements that differ between the two cases are the input matrices (derived from the respective historical datasets in Section 2) and the distribution parameters (identified in Section 3). This uniformity confirms that the proposed framework constitutes a general-purpose proof-of-concept methodology capable of representing diverse types of charging station utilization from a single, consistent modeling approach.

The proposed models operate at a temporal resolution of 15 min, corresponding to 96 simulation intervals per day. Historical connection-start times are assigned to quarter-hour slots by rounding their minute components to the nearest 15 min. Connection durations are expressed in hours and rounded to increments of 0.25 h. Charging sessions whose connection durations became zero after rounding were excluded from model development and were therefore not considered when constructing the corresponding connection-count and duration distributions. Consequently, these sessions do not contribute to the estimated connection frequencies or the simulated station occupancy. However, as the excluded sessions accounted for approximately 2% of the available historical records and represented very short connection durations, their exclusion was considered to have a negligible influence on the resulting station occupancy at the adopted temporal resolution. For the histogram-based duration model, empirical distributions are constructed separately for each arrival-time interval and day type. Histogram bin counts are determined from the available observations, and the resulting bin-center values are rounded to 0.25 h before being used for probabilistic sampling, as described by Equations (11) and (12).

The simulation is initialized at 00:00 on the first simulated day with all charging points available. The occupancy update mechanism tracks scheduled session completion times across consecutive simulation intervals, including sessions extending beyond midnight. The simulated station capacities are 20 charging points for the residential model and six charging points for the public model. The resulting stochastic simulations reproduce site-specific connection and occupancy patterns under the assumptions embedded in the historical data and simulation procedures. Further examination of alternative station capacities, changes in surrounding charging infrastructure, and user-behavior responses is necessary before extending the models to substantially different operating conditions.

5. Consistency Verification of the Generated Utilization Against the Calibration Data

The comparison in this section is a consistency verification of the complete generator, not an out-of-sample validation. The model is simulated for the same period and station size as the calibration data, and it is examined whether the generated connection-time profiles and connection durations reproduce those of the input data after passing through all model stages (Poisson sampling, capacity constraint, day-type switching and arrival-conditioned duration sampling). A chronological hold-out was not used because both datasets show pronounced changes in operating regime within the available records (Figures 1–3), so that a hold-out discrepancy would primarily reflect non-stationarity of the data rather than the modelling procedure. Out-of-sample validation on longer, stationary records is left for future work.

In this section, the comparison of the generated data with the input dataset is performed by comparing the whole dataset for the simulated period, which will allow us to evaluate whether the proposed model can represent the charging station utilization

after setting the distribution functions for the generation of the key parameters (number of connections and duration of connections). Additionally, this comparison will be used to determine whether the designed model can represent the input data, even if it has to ensure adherence to the data generation process concerning the type of day (workday, weekend). The charging station utilization is evaluated using the K-S test, histograms, and Q-Q plots, in the same way as for selecting the distributions to generate data.

5.1. Evaluation of the Residential Charging Station Utilization Model

The residential charging station utilization model evaluation was conducted for the simulation period from 15 July 2019 to 31 January 2020. This period was also used to construct matrices employed for data generation in the utilization model. The results from the K-S test are presented in Table 5. As expected, both key parameters did not reject the null hypothesis, due to the careful selection of appropriate distributions for data generation.

Table 5. Results of the Kolmogorov–Smirnov two-sample test for the number of connections and the duration of connections to the residential charging station.

Compared Data	h_0 at $\alpha = 0.05$	p	D
Number of connections	0	0.9992	0.052
Duration of connections	0	0.9919	0.061

Graphical evaluation through the histograms, as shown in Figures 27 and 28, indicates that both parameters exhibit minimal discrepancies compared to the real data. This suggests that the utilization model can generate data across the full spectrum of values present in the input dataset.

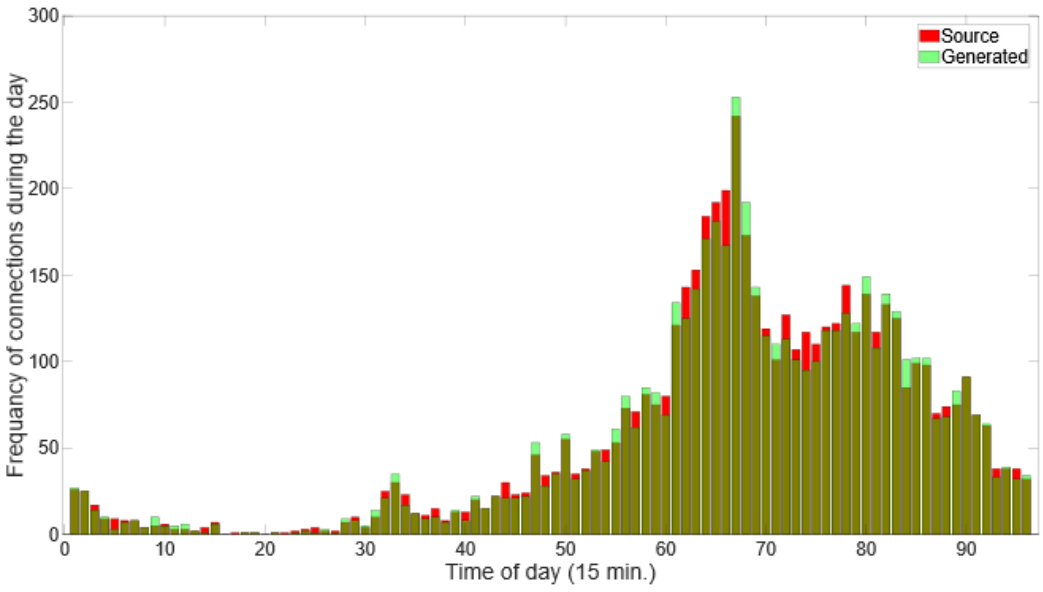


Figure 27. Histogram representing the comparison of generated data with input data for the number of connections during the simulated period in the residential charging station.

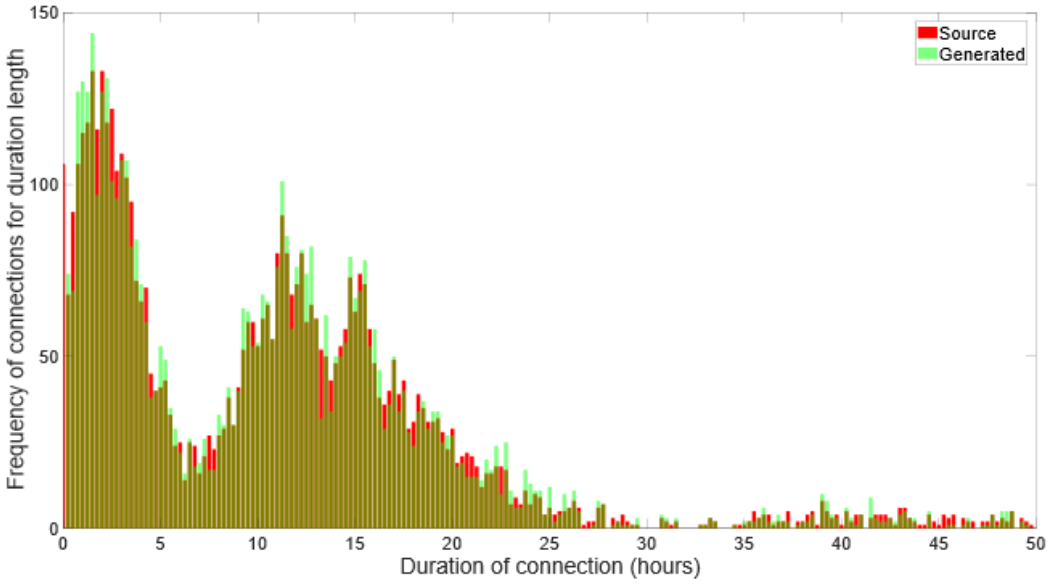


Figure 28. Histogram representing the comparison of generated data with input data for the duration of connections during the simulated period in the residential charging station.

The Q-Q plots presented in Figures 29 and 30 further corroborate these findings. The generated data for the number of connections closely mirrors the input dataset, as evidenced by the proximity of the points displayed to the reference line. However, for connection durations, some relative discrepancies are observed, with points deviating consistently from the reference line. This observation aligns with the results from the K-S test.

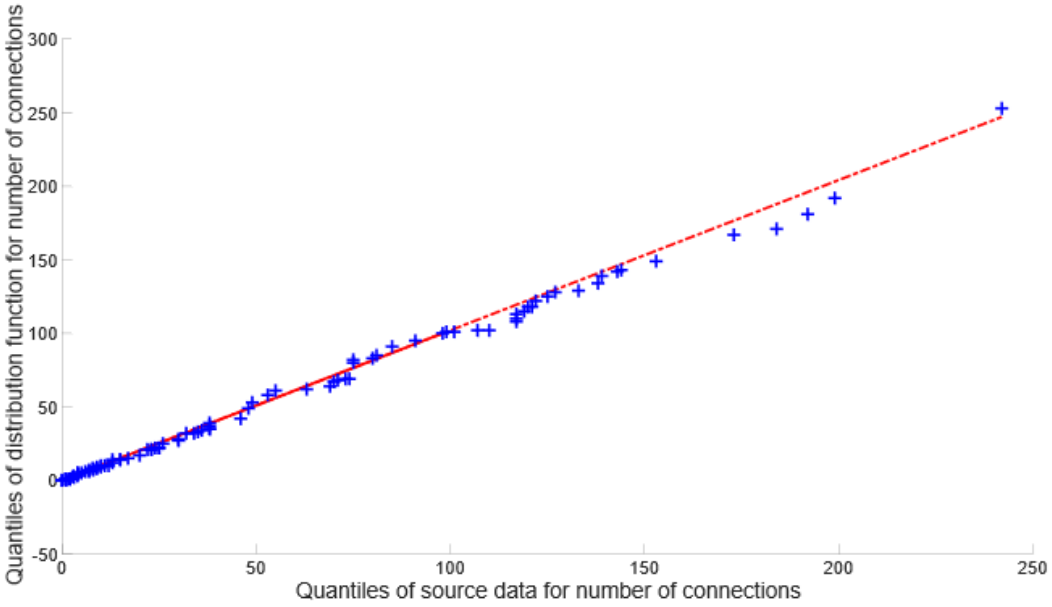


Figure 29. Q-Q plot representing the comparison of generated data with input data for the number of connections during the simulated period in the residential charging station.

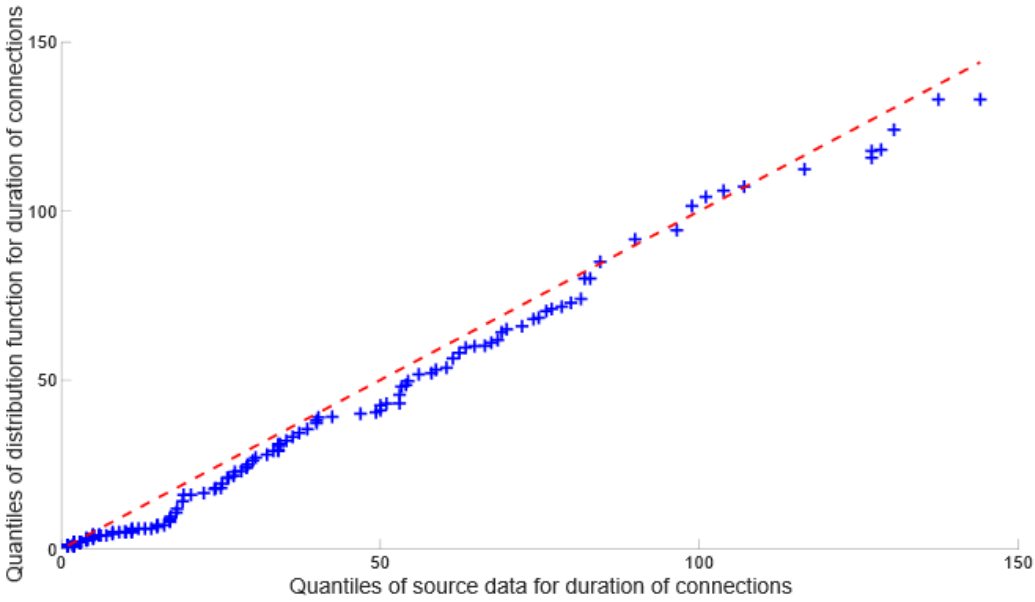


Figure 30. Q-Q plot representing the comparison of generated data with input data for the duration of connections during the simulated period in the residential charging station.

Overall, the evaluation demonstrates that the utilized generation method provides an accurate representation of the number of connections as well as connection durations for the residential charging station. It does not establish the accuracy of future occupancy trajectories or independent charging-demand predictions.

5.2. Evaluation of the Public Charging Station Utilization Model

The evaluation of the public charging station utilization model was performed for the period from January 2016 to January 2020. As with the residential charging station model, the simulation period corresponds to the period used for constructing the matrices employed in data generation. The initial comparison between the generated data and the input dataset was conducted using the K-S test, with results presented in Table 6. The findings show that neither generated parameter rejected the null hypothesis, with relatively high *p*-values observed.

Table 6. Results of the Kolmogorov–Smirnov two-sample test for the number of connections and the duration of connections to the public charging station.

Compared Data	h_0 at $\alpha = 0.05$	*p*	D
Number of connections	0	0.8789	0.083
Duration of connections	0	0.751	0.096

Histograms comparing the generated data with the input dataset are shown in Figures 31 and 32. These histograms indicate that the constructed utilization model is capable of generating data that spans the full range of values observed in the input dataset. Similar to the residential model, the generated data exhibits minimal discrepancies for both parameters.

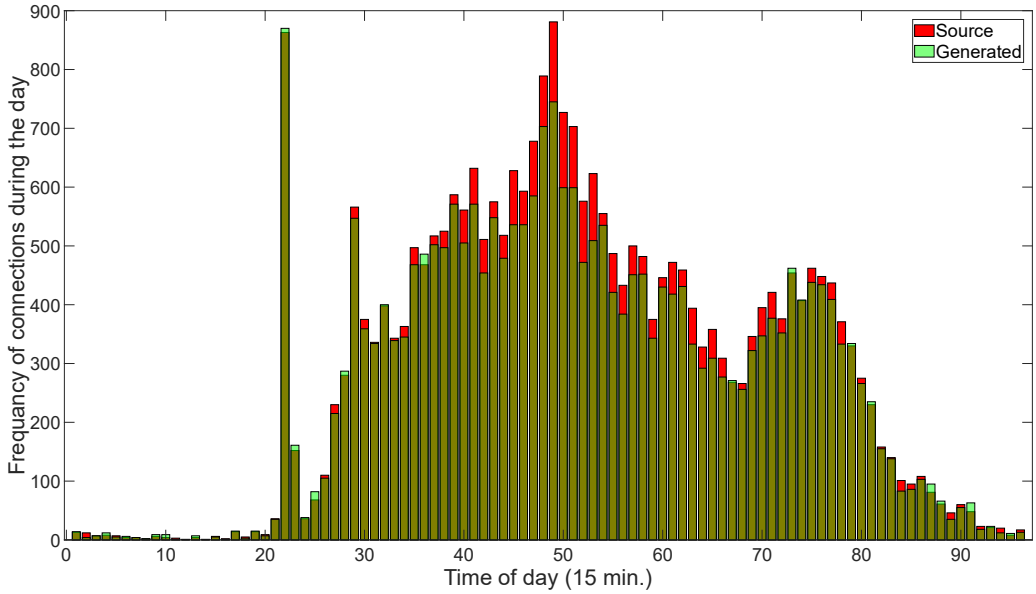


Figure 31. Histogram representing the comparison of generated data with input data for the number of connections during the simulated period in the public charging station.

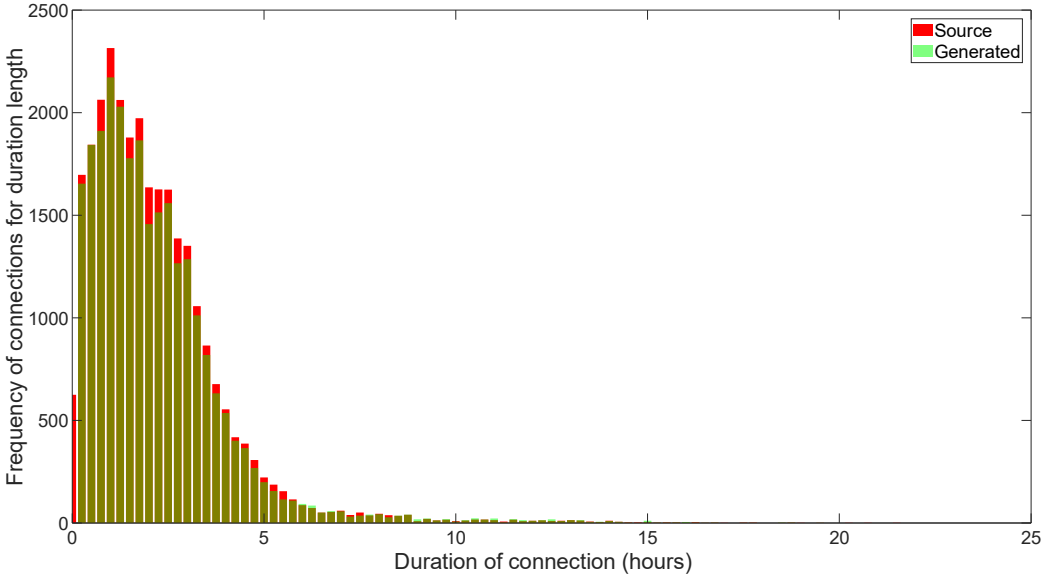


Figure 32. Histogram representing the comparison of generated data with input data for the duration of connections during the simulated period in the public charging station.

The Q-Q plots shown in Figures 33 and 34 reveal that the points, representing the comparison between the two datasets, are closely aligned with the reference line in both graphs. These results confirm the findings from the K-S test and histograms.

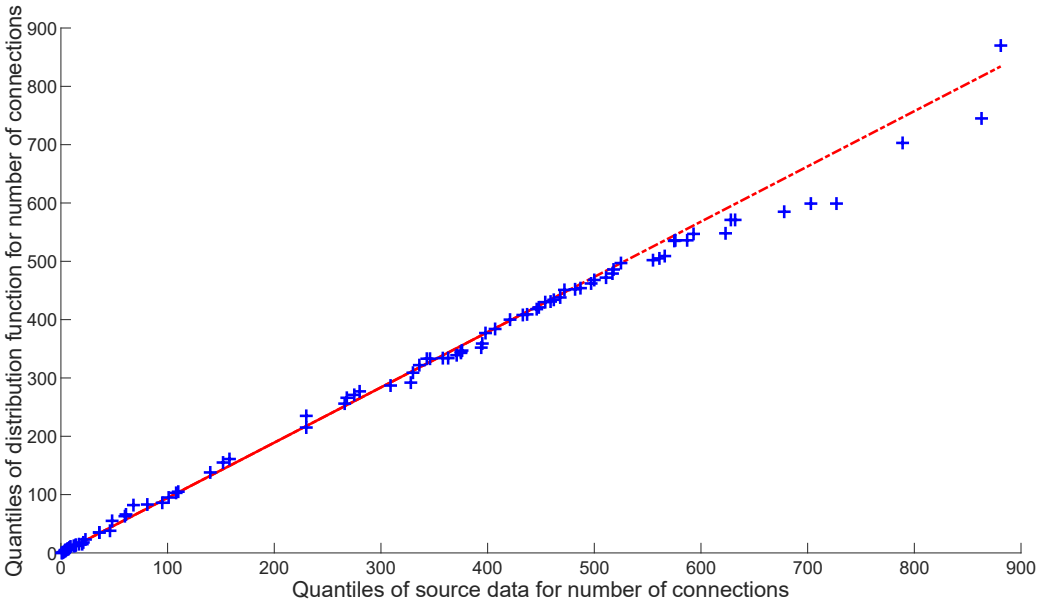


Figure 33. Q-Q plot representing the comparison of generated data with input data for the number of connections during the simulated period in the public charging station.

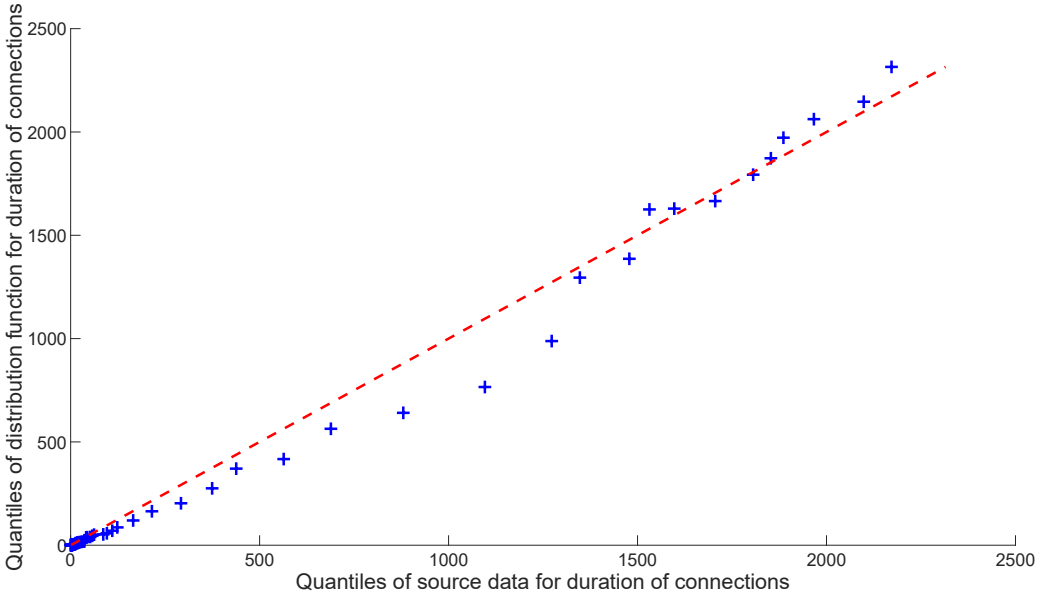


Figure 34. Q-Q plot representing the comparison of generated data with input data for the duration of connections during the simulated period in the public charging station.

Based on the results, it is evident that the generated data are consistent with the calibration data for both parameters; as noted above, this verifies the generator but does not constitute an out-of-sample validation.

6. Conclusions

The widespread adoption of EVs and associated charging infrastructure brings new challenges to the operation of the electrical network. An example of such a challenge may be increased power demand during peak demand times, increased demand volatility, or a decrease in power quality. Such challenges necessitate the creation and incorporation of advanced control strategies and intelligent solutions to mitigate the negative impacts of EV charging on the electrical network. To ensure these mechanisms are suitable and ready

for practical implementation, it is essential to evaluate them using models that can accurately simulate the operational behavior of charging stations.

Therefore, this paper presents a proof-of-concept stochastic model for electric vehicle charging station utilization at 15-minute resolution. The proposed methodology is based on historical charging data and combines dataset preparation, construction of connection and duration matrices, and probability-distribution-based data generation. The model was designed as a general framework that can be applied to different charging station types and datasets without changing the basic modelling structure. The methodology was verified on two publicly available datasets representing residential charging in Trondheim, Norway, and public charging in Palo Alto, California, USA. The results show that the proposed approach can reproduce the main statistical characteristics of real charging station operation while preserving its stochastic nature. For both sites, the generated connection-time profiles and connection-duration distributions were consistent with the calibration data. This shows that the generator reproduces the statistics it was calibrated on without distortion by the capacity constraint or the day-type switching; it does not by itself establish predictive accuracy for other periods or sites.

The proposed framework models the duration for which an EV remains physically connected to a charging point, rather than the duration of active battery charging. Consequently, station occupancy is determined by the plugged-in connection duration, regardless of whether energy is being transferred throughout this period. Active charging duration, charging power, and energy consumption are not explicitly modeled or evaluated. As the model relies on historical connection and disconnection records, the represented connection durations may also include idle periods during which the EV remains connected after charging has been completed. However, these periods are not explicitly distinguished from active charging periods within the proposed framework. Therefore, while the model can represent the overall duration of charging-point occupancy, it cannot independently determine the actual duration of energy transfer or the corresponding charging power demand. Incorporating an explicit distinction between active charging and idle connection periods represents a potential direction for future model development.

Furthermore, charging station utilization is influenced not only by user behavior but also by the availability, density, spatial distribution, and accessibility of charging infrastructure. Although the proposed model considers charging station capacity as a physical constraint, it does not explicitly account for the influence of surrounding charging infrastructure on charging demand and user preferences. These factors are implicitly reflected in the historical charging data used for model construction, as the recorded charging patterns represent the infrastructure conditions prevailing during the data collection period. Consequently, the resulting models are primarily representative of the specific charging environments from which the historical data originate and cannot directly predict changes in charging behavior resulting from infrastructure expansion or changes in charging accessibility. Nevertheless, the proposed methodology remains applicable to different infrastructure configurations, provided that corresponding historical charging data are available for model calibration.

The proposed model should be recalibrated when applied to charging stations or operating periods exhibiting substantially different charging patterns, including changes associated with user behavior, station utilization, or surrounding charging infrastructure. Calibration-period consistency alone does not establish predictive performance under such changed conditions.

The evaluation in Section 5 concerns the time-of-day profile of connections and the distribution of connection durations. Day-to-day overdispersion of arrivals, serial dependence beyond the daily rhythm, peak-occupancy statistics and rejection rates were

not assessed. As the Poisson arrival model does not represent day-level variability, it may understate the frequency of exceptionally busy days. A day-level Poisson–gamma mixture, which preserves the model structure, and comparison against Markov occupancy models are planned extensions.

The main purpose of the model is to serve as a proof of concept for future studies on charging-station operation, charging-control algorithms, and energy-management strategies. At the same time, the present implementation has several limitations, including the absence of explicit seasonal effects, longer-term behavioral changes, and finer temporal resolution below 15 min. Future work will therefore focus on extending the model with additional influencing factors, improving its adaptability to other charging environments, and validating it on further datasets.

Author Contributions: Conceptualization, M.T.; Data curation, M.T. and F.P.; methodology, M.T.; software, M.T.; validation, M.H., P.K.; writing—original draft preparation, M.T. and F.P.; writing—review and editing, M.H. and P.K. All authors have read and agreed to the published version of the manuscript.

Funding: This research received no external funding.

Data Availability Statement: The original data presented in the study are openly available in Mendeley Data at DOI: 10.17632/jbks2rcwyj.1 and in Palo Alto Open Data Portal at https://data.paloalto.gov/datasets/194693/electric-vehicle-charging-station-usage-july-2011-dec-2020/ (accessed on 10 April 2026).

Acknowledgments: During the preparation of this manuscript, the authors used ChatGPT, version 5.6 Sol, for the purpose of grammar checks and text polishing. The authors have reviewed and edited the output and take full responsibility for the content of this publication.

Conflicts of Interest: The authors declare no conflicts of interest.

Abbreviations

The following abbreviations are used in this manuscript:

A	Number of charging stands
A-D test	Anderson–Darling test
A_{itr}	Number of available charging spaces during simulation
b	Number of bins in the histogram
CDF	Cumulative Distribution Function
$C_{EVbattery}$	Value of EV nominal battery capacity for connected EV
C_{wd}	Vector of all connection times during workdays
D	Two-sample K-S test statistics
D_{wd}	Vector of workdays dates during the selected period
d_{wd}	Date from the vector of workday dates D_{wd}
EV	Electric Vehicle
h	Connection duration generated for each EV connected to the charging station
h_0	Indication of null hypothesis rejections in K-S test, test decision at $\alpha = 0.05$ (1 = h_0 rejected)
$\boldsymbol{H_{wd}}$	Matrix representing the duration of connections
h_{wd}	Generated duration of EV connection to the charging station from histogram values defined from real data for workdays
K-S test	Kolmogorov–Smirnov test
K_{wd}	Vector of connection duration times during workdays
k_{wd}	Connection duration time from the vector of connection duration times during the workdays in the selected period (K_{wd})
L_{wd}	Vector of all connection duration times during workdays
n	Number of EV connections to the charging station

$\boldsymbol{N_{wd}}$	Matrix representing the number of EV connections during workdays
n_{wd}	Number of connected EVs generated from the distribution function based on the real data for workdays/weekends
p	p-value of the two-sample K-S test
$p_{wd,i}$	probability of selecting the i-th value from the histogram generated from matrix Hwd
Q	Number of days during the simulation period
SoC	State of Charge
T	Time vector
t	Time from the time vector T
t_e	End date for the simulation period
t_s	Start date for the simulation period
T_{sim}	Simulation period in days
t_{sim}	Date value in the simulation period
u_{wd}	Number of matches in vector v_{wd}
W_{wd}	Vector of all connection dates during workdays
x_{EV0}	EV battery SoC when connected to the charging station
δ_{wd}	Vector of logical values representing matches between the date d_{wd} and dates in W_{wd}
κ_{wd}	Values of the histogram generated from matrix $\boldsymbol{H_{wd}}$
λ	Lambda parameter of the Poisson distribution function
μ_{wd}	Intersection of values matching both the date d_{wd} and time t
ξ_{wd}	frequency of values in the histogram generated from matrix $\boldsymbol{H_{wd}}$
σ_{wd}	Value of the corresponding 15-min period of the day in which the EV was connected to the charging station when the matched connection duration time was measured during workdays/weekends
τ_{wd}	Vector of logical values representing matches between each time t and the connection times in C_{wd}
v_{wd}	Vector of logical values representing matches between the duration time k_{wd} and duration times within the vector L_{wd}

Appendix A

Table A1. Number of retained duration observations for each 15-min time interval and day type for residential charging station dataset.

Time Interval	Observed Weekdays	Weekday Duration Sessions	Observed Weekend Days	Weekend Duration Sessions
00:00:00	145	18	56	8
00:15:00	145	9	56	16
00:30:00	145	7	56	10
00:45:00	145	7	56	2
01:00:00	145	6	56	3
01:15:00	145	4	56	4
01:30:00	145	4	56	4
01:45:00	145	1	56	3
02:00:00	145	2	56	3
02:15:00	145	2	56	4
02:30:00	145	2	56	1
02:45:00	145	0	56	3
03:00:00	145	1	56	1
03:15:00	145	1	56	3
03:30:00	145	1	56	6
03:45:00	145	0	56	0
04:00:00	145	1	56	0
04:15:00	145	0	56	1
04:30:00	145	0	56	1
04:45:00	145	0	56	0

05:00:00	145	1	56	0
05:15:00	145	0	56	1
05:30:00	145	0	56	2
05:45:00	145	3	56	0
06:00:00	145	2	56	2
06:15:00	145	0	56	2
06:30:00	145	1	56	1
06:45:00	145	7	56	0
07:00:00	145	9	56	1
07:15:00	145	4	56	0
07:30:00	145	10	56	0
07:45:00	145	22	56	3
08:00:00	145	25	56	5
08:15:00	145	18	56	5
08:30:00	145	11	56	1
08:45:00	145	7	56	4
09:00:00	145	10	56	5
09:15:00	145	8	56	0
09:30:00	145	10	56	3
09:45:00	145	8	56	5
10:00:00	145	17	56	3
10:15:00	145	12	56	3
10:30:00	145	16	56	6
10:45:00	145	18	56	12
11:00:00	145	16	56	7
11:15:00	145	12	56	12
11:30:00	145	24	56	15
11:45:00	145	24	56	10
12:00:00	145	25	56	11
12:15:00	145	33	56	22
12:30:00	145	19	56	16
12:45:00	145	21	56	17
13:00:00	145	30	56	18
13:15:00	145	25	56	22
13:30:00	145	30	56	22
13:45:00	145	40	56	33
14:00:00	145	45	56	26
14:15:00	145	51	56	29
14:30:00	145	45	56	29
14:45:00	145	55	56	24
15:00:00	145	77	56	43
15:15:00	145	94	56	48
15:30:00	145	112	56	41
15:45:00	145	155	56	27
16:00:00	145	163	56	29
16:15:00	145	174	56	24
16:30:00	145	208	56	31
16:45:00	145	130	56	41
17:00:00	145	100	56	38
17:15:00	145	82	56	37
17:30:00	145	65	56	36
17:45:00	145	88	56	37
18:00:00	145	81	56	26

18:15:00	145	82	56	35
18:30:00	145	77	56	33
18:45:00	145	82	56	38
19:00:00	145	85	56	37
19:15:00	145	113	56	31
19:30:00	145	98	56	17
19:45:00	145	101	56	37
20:00:00	145	98	56	19
20:15:00	145	104	56	28
20:30:00	145	105	56	20
20:45:00	145	69	56	16
21:00:00	145	72	56	26
21:15:00	145	81	56	17
21:30:00	145	59	56	10
21:45:00	145	55	56	19
22:00:00	145	58	56	15
22:15:00	145	68	56	23
22:30:00	145	52	56	17
22:45:00	145	51	56	11
23:00:00	145	30	56	8
23:15:00	145	32	56	6
23:30:00	145	25	56	13
23:45:00	145	22	56	10

Table A2. Number of retained duration observations for each 15-min time interval and day type for the public charging station dataset.

Time Interval	Observed Weekdays	Weekday Duration Sessions	Observed Weekend Days	Weekend Duration Sessions
00:00:00	1032	8	411	5
00:15:00	1032	5	411	4
00:30:00	1032	6	411	1
00:45:00	1032	5	411	3
01:00:00	1032	3	411	4
01:15:00	1032	1	411	3
01:30:00	1032	4	411	0
01:45:00	1032	1	411	1
02:00:00	1032	3	411	3
02:15:00	1032	2	411	1
02:30:00	1032	1	411	2
02:45:00	1032	1	411	0
03:00:00	1032	3	411	1
03:15:00	1032	1	411	0
03:30:00	1032	5	411	1
03:45:00	1032	2	411	0
04:00:00	1032	13	411	0
04:15:00	1032	5	411	0
04:30:00	1032	13	411	0
04:45:00	1032	9	411	0
05:00:00	1032	34	411	1
05:15:00	1032	847	411	3
05:30:00	1032	149	411	0
05:45:00	1032	33	411	1

06:00:00	1032	64	411	4
06:15:00	1032	105	411	4
06:30:00	1032	224	411	5
06:45:00	1032	268	411	8
07:00:00	1032	533	411	27
07:15:00	1032	333	411	40
07:30:00	1032	285	411	43
07:45:00	1032	246	411	139
08:00:00	1032	265	411	71
08:15:00	1032	268	411	90
08:30:00	1032	395	411	101
08:45:00	1032	337	411	125
09:00:00	1032	321	411	193
09:15:00	1032	337	411	184
09:30:00	1032	382	411	197
09:45:00	1032	320	411	231
10:00:00	1032	366	411	257
10:15:00	1032	290	411	213
10:30:00	1032	342	411	223
10:45:00	1032	319	411	191
11:00:00	1032	390	411	217
11:15:00	1032	360	411	219
11:30:00	1032	438	411	215
11:45:00	1032	548	411	226
12:00:00	1032	639	411	226
12:15:00	1032	501	411	214
12:30:00	1032	480	411	203
12:45:00	1032	406	411	153
13:00:00	1032	448	411	162
13:15:00	1032	404	411	127
13:30:00	1032	379	411	92
13:45:00	1032	332	411	88
14:00:00	1032	409	411	76
14:15:00	1032	386	411	83
14:30:00	1032	308	411	58
14:45:00	1032	355	411	83
15:00:00	1032	395	411	69
15:15:00	1032	393	411	55
15:30:00	1032	334	411	48
15:45:00	1032	282	411	41
16:00:00	1032	280	411	65
16:15:00	1032	233	411	66
16:30:00	1032	197	411	61
16:45:00	1032	208	411	50
17:00:00	1032	273	411	68
17:15:00	1032	316	411	71
17:30:00	1032	327	411	84
17:45:00	1032	281	411	84
18:00:00	1032	334	411	104
18:15:00	1032	312	411	88
18:30:00	1032	353	411	87
18:45:00	1032	347	411	81
19:00:00	1032	335	411	83

19:15:00	1032	283	411	74
19:30:00	1032	261	411	54
19:45:00	1032	202	411	61
20:00:00	1032	172	411	47
20:15:00	1032	115	411	39
20:30:00	1032	108	411	26
20:45:00	1032	67	411	25
21:00:00	1032	68	411	20
21:15:00	1032	72	411	30
21:30:00	1032	66	411	13
21:45:00	1032	47	411	9
22:00:00	1032	36	411	7
22:15:00	1032	46	411	13
22:30:00	1032	35	411	10
22:45:00	1032	17	411	5
23:00:00	1032	17	411	3
23:15:00	1032	11	411	9
23:30:00	1032	8	411	0
23:45:00	1032	11	411	4

References

1. Almatar, K.M. Increasing electric vehicles infrastructure in urban areas for efficiently employing renewable energy. *Environ. Dev. Sustain.* **2024**, *26*, 26183–26204. https://doi.org/10.1007/s10668-023-03723-x.
2. Xia, X.; Li, P.; Xia, Z.; Wu, R.; Cheng, Y. Life cycle carbon footprint of electric vehicles in different countries: A review. *Sep. Purif. Technol.* **2022**, *301*, 122063. https://doi.org/10.1016/j.seppur.2022.122063.
3. Li, P.; Xia, X.; Guo, J. A review of the life cycle carbon footprint of electric vehicle batteries. *Sep. Purif. Technol.* **2022**, *296*, 121389. https://doi.org/10.1016/j.seppur.2022.121389.
4. Morfeldt, J.; Johansson, D.J.A. Impacts of shared mobility on vehicle lifetimes and on the carbon footprint of electric vehicles. *Nat. Commun.* **2022**, *13*, 6400. https://doi.org/10.1038/s41467-022-33666-2.
5. Leou, R.-C.; Teng, J.-H.; Su, C.-L. Modelling and verifying the load behaviour of electric vehicle charging stations based on field measurements. *IET Gener. Transm. Distrib.* **2015**, *9*, 1112–1119. https://doi.org/10.1049/iet-gtd.2014.0446.
6. Heymann, F.; Pereira, C.; Miranda, V.; Soares, F.J. Spatial load forecasting of electric vehicle charging using GIS and diffusion theory. In *2017 IEEE PES Innovative Smart Grid Technologies Conference Europe (ISGT-Europe)*; IEEE: New York, NY, USA, 2017; pp. 1–6. https://doi.org/10.1109/ISGTEurope.2017.8260172.
7. Buzna, L.; De Falco, P.; Khormali, S.; Proto, D.; Straka, M. Electric vehicle load forecasting: A comparison between time series and machine learning approaches. In *2019 1st International Conference on Energy Transition in the Mediterranean Area (SyNERGY MED)*; IEEE: New York, NY, USA, 2019; pp. 1–5. https://doi.org/10.1109/SyNERGY-MED.2019.8764110.
8. Kene, R.O.; Olwal, T.O. Energy Management and Optimization of Large-Scale Electric Vehicle Charging on the Grid. *World Electr. Veh. J.* **2023**, *14*, 95. https://doi.org/10.3390/wevj14040095.
9. Bayram, I.S.; Ismail, M. A Stochastic Model for Fast Charging Stations with Energy Storage Systems. In *2019 IEEE Transportation Electrification Conference and Expo (ITEC)*; IEEE: New York, NY, USA, 2019; pp. 1–5. https://doi.org/10.1109/ITEC.2019.8790570.
10. Alizadeh, M.; Moradi Amani, A.; Meegahapola, L.; Jalili, M.; Hill, O. Optimal Traffic-Informed Design and Operation of EV Charging Stations in Power Distribution Grids. *IEEE Trans. Transp. Electrif.* **2026**, *12*, 4375–4387. https://doi.org/10.1109/TTE.2026.3670484.
11. Alizadeh, M.; Amani, A.M.; Meegahapola, L.; Jalili, M.; Hill, O. Optimal Integration of EV Charging Stations into Distribution Network Planning and Operation. *IEEE Trans. Ind. Inform.* **2025**, *21*, 7120–7130. https://doi.org/10.1109/TII.2025.3574435.
12. Da Costa Mendes, P.R.; Normey-Rico, J.E.; Alba, C.B. Economic energy management of a microgrid including electric vehicles. In *2015 IEEE PES Innovative Smart Grid Technologies Latin America (ISGT LATAM)*; IEEE: New York, NY, USA, 2015; pp. 869–874. https://doi.org/10.1109/ISGT-LA.2015.7381269.
13. Chen, C.; Duan, S. Microgrid economic operation considering plug-in hybrid electric vehicles integration. *J. Mod. Power Syst. Clean Energy* **2015**, *3*, 221–231. https://doi.org/10.1007/s40565-015-0116-0.

14. Mendes, P.R.C.; Normey-Rico, J.E.; Bordons, C. Distributed Energy Management System for V2G Networked Microgrids. In *2017 IEEE PES Innovative Smart Grid Technologies Conference—Latin America (ISGT Latin America)*; IEEE: New York, NY, USA, 2017; pp. 1–6. https://doi.org/10.1109/ISGT-LA.2017.8126700.
15. Yan, J.; Menghwar, M.; Asghar, E.; Kumar Panjwani, M.; Liu, Y. Real-time energy management for a smart-community microgrid with battery swapping and renewables. *Appl. Energy* **2019**, *238*, 180–194. https://doi.org/10.1016/j.apenergy.2018.12.078.
16. Liao, J.T.; Lin, C.I.; Chien, C.Y.; Yang, H.T. The distributed energy resources operation for EV charging stations and SHEMS in microgrids. In *2014 International Conference on Intelligent Green Building and Smart Grid (IGBSG)*; IEEE: New York, NY, USA, 2014; pp. 1–6. https://doi.org/10.1109/IGBSG.2014.6835256.
17. Engelhardt, J.; Zepter, J.M.; Gabderakhmanova, T.; Marinelli, M. Energy management of a multi-battery system for renewable-based high power EV charging. *eTransportation* **2022**, *14*, 100198. https://doi.org/10.1016/j.etran.2022.100198.
18. Srilakshmi, E.; Singh, S.P. Energy regulation of EV using MILP for optimal operation of incentive based prosumer microgrid with uncertainty modelling. *Int. J. Electr. Power Energy Syst.* **2022**, *134*, 107353. https://doi.org/10.1016/j.ijepes.2021.107353.
19. Wang, T.; O'Neill, D.; Kamath, H. Dynamic Control and Optimization of Distributed Energy Resources in a Microgrid. *IEEE Trans. Smart Grid* **2015**, *6*, 2884–2894. https://doi.org/10.1109/TSG.2015.2430286.
20. Rajamand, S. Feedback-based control structure for frequency/voltage regulation using the state of electrical vehicle charge station and point estimation method. *Sustain. Energy Technol. Assess.* **2022**, *51*, 101922. https://doi.org/10.1016/j.seta.2021.101922.
21. Yuan, H.; Wei, G.; Zhu, L.; Zhang, X.; Zhang, H.; Luo, Z. Optimal scheduling for micro-grid considering EV charging–swapping–storage integrated station. *IET Gener. Transm. Distrib.* **2020**, *14*, 1127–1137. https://doi.org/10.1049/iet-gtd.2018.6912.
22. Soares, F.J.; Peças Lopes, J.A.; Rocha Almeida, P.M.; Moreira, C.L.; Seca, L. A stochastic model to simulate electric vehicles motion and quantify the energy required from the grid. In Presented at the 17th Power Systems Computation Conference, PSCC, Stockholm, Sweden, 22–26 August 2011.
23. Sørensen, Å.L. Residential electric vehicle charging datasets from apartment buildings. *Data Brief* **2021**, *36*, 107105. https://doi.org/10.17632/jbks2rcwyj.1.
24. "Electric Vehicle Charging Station Usage (July 2011–Dec 2020) · Open Data · City of Palo Alto," City of Palo Alto. Available online: http://data.paloalto.gov/datasets/194693/electric-vehicle-charging-station-usage-july-2011-dec-2020/ (accessed on 10 April 2026).

Disclaimer/Publisher's Note: The statements, opinions and data contained in all publications are solely those of the individual author(s) and contributor(s) and not of MDPI and/or the editor(s). MDPI and/or the editor(s) disclaim responsibility for any injury to people or property resulting from any ideas, methods, instructions or products referred to in the content.